SunQM-6s7: The Face-to-face Tidal-locked Binary Orbital Rotation May Be the Origin of the Electron Spin and the Nucleon Spin

Yi Cao

e-mail: yicaojob@yahoo.com. ORCID: 0000-0002-4425-039X

Abstract

1) Many QM text books showed that the matter wave has the relationship of $v_{n,ph} = \frac{1}{2}v_{n,gr}$, my research result suggested that $v_{n,ph} = \frac{n}{2}v_{n,gr}$ may be the more Eigen description. My research result revealed that the non-Born probability (NBP) or de Broglie wave can be used for either the group wave, or the phase wave. My research result also revealed that it is the phase wave that reflects each single electron/object's true matter wave property, the group wave only reflects the property of all electrons/objects as a group. 2) The paired up/down spin information of the electron and the nucleon may have already been presented by the positive/negative wave peaks (of the phase wave) in either the Schrodinger equation/solution (in form of NBP), or in the de Broglie wave in the Bohr H-atom model. 3) The spin of both the electron and the nucleon (in an atom) may originate from the face-to-face tidal-locked binary circular orbital rotation between them. This hypothesis also perfectly fits to the new "proton-electron mirror-coupled orbit" model (in SunQM-6s6). The result of Bohr-QM formula $L_{n,orbit} = mv_nr_n = n\hbar$ may directly support this hypothesis. 4) Ultimately, the real meaning of spin ½$\hbar$ for an electron may be: the electron always has an effective orbital angular momentum (between the inner and outer edges of the n shell) that is ½$\hbar$ higher than the value at the inner edge of the n orbit. And because of the face-to-face tidal-locked, this ½$\hbar$ effective orbital angular momentum is carried over by the electron as the electron's effective spin angular momentum. 5) For a pair of spin up/down electrons, their (electron-proton face-to-face tidal-locked) orbital movement in φ-1D (in the opposite ±m directions) may have transformed into a uni-directional orbital movement in θ-1D. 6) A spin configuration for each of the four nucleons in an alpha particle has been proposed. 7) Planets' spin origin may also can be explained by using the similar Bohr-QM formula $L_{n,orbit} = mv_nr_n = n\hbar_{gen}$ (that is specified for the Solar system). 8) This analysis again showed that, the quantum phenomenon is produced by the interference of the 3D spherical wave of a point-centered field (of force, mass, energy, etc.) to become a spherical 3D wave packet, so that the NBP (= wave) peaks at some positions and valleys at some other positions.

Key Words: Quantum mechanics, {N,n} QM, Schrodinger equation, spin.

Introduction

In August 2016, I discovered that the Solar system follows a brand new {N,n//6} quantum mechanical structure [1]. Based on that result, (during the 10 years of the closed-door research), I further (independently) developed the {N,n} QM theory, and showed that not only the formation of Solar system [1] ~ [16], but also the formation of the whole universe [17] ~ [25], may can be described by the {N,n} QM. (Note: As an independent scientist, some of my research work may belong to a citizen scientist leveled work). As part of the {N,n} QM development, I (independently) designed a completely new {N,n} QM field theory [23] ~[24], [26] ~ [30]. The foundation of this theory includes: the four fundamental forces (Gravity, Electromagnetic, Strong, Weak, abbreviated as G-, E/M-, S-, W-forces) have been re-classified into three pairs of force

(E/RFe-force, G/RFg-force; S/RFs-force, see SunQM-6); all point-centered fields (including the mass field, the force field, and the energy field) can be represented by the Schrodinger equation/solution (in form of non-Born probability as well as in the form of 3D spherical wave packet, see SunQM-6s4); the non-Born probability description that equals to the re-explanation of the Born probability density as the collection of all elliptical orbital tracks (or, the Born probability density map's contour lines can be re-explained as the trajectory of the motion electron, see SunQM-6s2's Fig-2), the 3D wave packet description and the dis-entanglement of the outmost shell (i.e., the "general decaying" process, see SunQM-6s1, -6s2, -6s3), the "|nL0> elliptical/parabolic/hyperbolic orbital transition model" (see SunQM-6s2, -6s3), and the trick that using the high-frequency n' quantum number to pin-point any small region in the {N,n} QM field (see SunQM-3s11, -6s1, etc.). In the current paper, I hypothesized that the spin of both electron and nucleon may be originated from the face-to-face tidal-locked binary circular orbital motion between them. Some preliminary evidences have been explained here.

Note: QM means Quantum Mechanics. For {N,n} QM nomenclature as well as the general notes, please see SunQM-1's sections VII & VIII. Note: Microsoft Excel's number format is often used in this paper, for example: x^2 = x^2, 3.4E+12 = 3.4*10^{12} = 3.4×10^{12}, 5.6E-9 = 5.6*10^{-9}. Note: The easiest reading sequence for the (30 posted) SunQM series papers is: SunQM-1, 1s1, 1s2, 1s3, 2, 3, 3s1, 3s2, 3s6, 3s7, 3s8, 3s3, 3s9, 3s4, 3s10, 3s11, 4, 4s1, 4s2, 5, 5s1, 5s2, 7, 6, 6s1, 6s2, 6s3, 6s4, 6s5, and 6s6. Note: for all SunQM series papers, reader should check "SunQM-9s1: Updates and Q/A for SunQM series papers" for the most recent updates and corrections. Note: |n*l*m> means |n,*l*,m> QM state, "nLL" or |nLL> means |n,*l*,m> QM state with *l* = n-1 = L, and *m* = n-1 = L. "nL0" or |nL0> means |n,*l*,m> QM state with *l* = n-1 = L, and m = 0. Note: In the current paper, the cited SunQM series numbers of those pre-posted SunQM papers may not be the final SunQM series numbers (after posting), so, readers may need to match the right SunQM series number (for those pre-posting SunQM papers after they are posted, according to the list of "A series of SunQM papers that I am working on" at the end of current paper) before reading those (pre-posted) citations.

I. Re-deduce the relationship between phase wave and group wave parameters by using $v_{n,ph} = \frac{n}{2} v_{n,gr}$, and then the $v_{ph} = \frac{1}{2} v_{gr}$ in QM text books may need to be replaced accordingly

In many QM text books [31] ~ [32], a matter wave's phase velocity and group velocity were described as $v_{n,ph} = \frac{1}{2} v_{n,gr}$, and I had used this relationship for deducing the (bound state) orbital movement of the group wave and the phase wave (see SunQM-6s1's eq-1 though eq-26). However, when I tried to used that result for constructing Table 1, the general physical rule of the orbital angular frequency $\omega_{n,ph} = v_{n,ph} / r_n$ become not applicable. This means, SunQM-6s1's eq-1 though eq-26 are not the Eigen description in physics. On the other hand, in SunQM-4's work, I already realized that $\omega_{n,ph} = \frac{n}{2} \omega_{n,gr}$ (see SunQM-4's eq-40) must be a more generalized form of $\omega_{n,ph} = \frac{1}{2} \omega_{n,gr}$ (see SunQM-4's eq-41). Based on that, now I start to believe that $v_{n,ph} = \frac{n}{2} v_{n,gr}$, (rather than $v_{n,ph} = \frac{1}{2} v_{n,gr}$), is the more Eigen description for matter wave's (bound state) orbital motion. Therefore, I re-did the deduction, and the result was shown in eq-1 through eq-21 below. (Note: the following deduction are based on $v_{n,ph} = \frac{n}{2} v_{n,gr}$).

$v_{n,ph} = \frac{n}{2} v_{n,gr}$, based on SunQM-4's eq-40, and from my "first principle thinking" eq-1

$\lambda_{n,gr} = 2\pi r_n / n$ or $2\pi r_n = n\lambda_{n,gr}$, From Bohr-de Broglie's 1D circular orbit QM eq-2

$v_{n,gr} = 2\pi r_n f_{n,gr} = n\lambda_{n,gr} f_{n,gr}$, from the definition of the wave mechanics, and using eq-2 eq-3

$v_{n,gr} = \frac{v_{1,gr}}{n}$ from Bohr QM eq-4

$v_{n,ph} = v_{1,ph}$, eq-5

deduced from $v_{n,ph} = \frac{n}{2} v_{n,gr} \rightarrow v_{1,ph} = \frac{1}{2} v_{1,gr}$, $v_{n,gr} = \frac{v_{1,gr}}{n}$, $v_{n,ph} = \frac{n}{2} v_{n,gr} = \frac{n}{2}\frac{v_{1,gr}}{n} = \frac{1}{2} v_{1,gr} = v_{1,ph}$

$\lambda_{n,gr} = n\lambda_{1,gr}$, deduced from $\lambda_{n,gr} = \frac{2\pi r_n}{n} = \frac{2\pi r_1 n^2}{n} = 2\pi r_1 n = n\lambda_{1,gr}$, eq-6

or, $\lambda_{n,gr} = 2\pi r_1 n$, $\lambda_{n,gr} = \frac{2\pi r_n}{n}$, or, $n\lambda_{n,gr} = 2\pi r_n$ eq-7

$\lambda_{n,ph} = n^2 \lambda_{1,ph}$, or, $\lambda_{n,ph} = 2\pi r_1 n^2$ eq-8

deduced from $v_{n,ph} = v_{1,ph} \rightarrow \lambda_{n,ph} f_{n,ph} = \lambda_{1,ph} f_{1,ph}$, $\lambda_{n,ph} = \lambda_{1,ph} \frac{f_{1,ph}}{f_{n,ph}} = n^2 \lambda_{1,ph}$

$\lambda_{n,ph} = 2\pi r_n$, deduced from $\lambda_{n,ph} = 2\pi r_1 n^2 = 2\pi r_n$, this correlates to $v_{n,ph} = v_{1,ph}$ eq-9

$v_{n,ph} = \lambda_{n,ph} f_{n,ph}$, from the definition of the wave mechanics, or, $v_{n,ph} = 2\pi r_n f_{n,ph}$ eq-10

$\lambda_{n,ph} = n\lambda_{n,gr}$, deduced from $\lambda_{n,ph} = 2\pi r_n = n\lambda_{n,gr}$ eq-11

$f_{n,ph} = \frac{f_{1,ph}}{n^2}$, eq-12

deduced from , $v_{n,ph} = 2\pi r_n f_{n,ph} = \lambda_{n,ph} f_{n,ph} = v_{1,ph} = 2\pi r_1 f_{1,ph} \rightarrow r_n f_{n,ph} = r_1 f_{1,ph} \rightarrow f_{n,ph} = \frac{r_1}{r_n} f_{1,ph} = \frac{f_{1,ph}}{n^2}$, This is expected, because it must satisfy the wave energy formula for a photon:

$E_n - E_{n'} = -Hmf_{n,ph} - (-Hmf_{n',ph}) = -Hmf_{1,ph}\left(\frac{1}{n^2} - \frac{1}{n'^2}\right)$ eq-13

$f_{n,ph} = \frac{n}{2} f_{n,gr}$, deduced $v_{n,ph} = \frac{n}{2} v_{n,gr} \rightarrow \lambda_{n,ph} f_{n,ph} = \frac{n}{2}(n\lambda_{n,gr}) f_{n,gr} = \frac{n}{2}(\lambda_{n,ph}) f_{n,gr}$ eq-14

$f_{n,gr} = \frac{f_{1,gr}}{n^3}$, eq-15

deduced from $v_{n,gr} = n\lambda_n f_{n,gr}$ & $v_{1,gr} = \lambda_1 f_{1,gr}$ & $v_{n,gr} = \frac{v_{1,gr}}{n}$, $n\lambda_n f_{n,gr} = \frac{\lambda_1 f_{1,gr}}{n}$, $nn\lambda_1 f_{n,gr} = \frac{\lambda_1 f_{1,gr}}{n}$, this is completely unexpected, but it has been confirmed by the pseudo n orbit number calculation (in SunQM-6s1's Fig-1a): Define $f_{3,ph} - f_{2,ph} = -f_{n,gr}$, use $f_{n,ph} = \frac{f_{1,ph}}{n^2}$, $f_{n,ph} = \frac{n}{2} f_{n,gr}$, and $f_{n,gr} = \frac{f_{1,gr}}{n^3}$, $f_{3,ph} - f_{2,ph} = f_{1,ph}\left(\frac{1}{3^2} - \frac{1}{2^2}\right) = \left(\frac{1}{2}\right) f_{1,gr}\left(\frac{1}{3^2} - \frac{1}{2^2}\right) = -f_{n,gr} = -\frac{f_{1,gr}}{n^3}$, $\frac{1}{n^3} = \left(\frac{1}{2}\right)\left(\frac{1}{2^2} - \frac{1}{3^2}\right)$, $n \approx 2.433$.

$\omega_{n,gr} = 2\pi f_{n,gr} = v_{n,gr} / r_n$, eq-16

$\omega_{n,ph} = 2\pi f_{n,ph} = v_{n,ph} / r_n = (n/2) v_{n,gr} / r_n$, eq-17

$\omega_{n,ph} = (n/2)\omega_{n,gr}$, or, $f_{n,ph} = (n/2) f_{n,gr}$, eq-18

To confirm:

$v_{1,gr} = n v_{n,gr} = n(n\lambda_{n,gr} f_{n,gr}) = n^2 n\lambda_{1,gr} \frac{f_{1,gr}}{n^3} = \lambda_{1,gr} f_{1,gr} = v_{1,gr}$, correct.

$v_{n,ph} = 2\pi r_n f_{n,ph} = \lambda_{n,ph} f_{n,ph} = n^2 \lambda_{1,ph} \frac{f_{1,ph}}{n^2} = \lambda_{1,ph} f_{1,ph} = v_{1,ph}$, correct.

Under {N,n} QM, a mass body's momentum p_n has a de Broglie matter wave :

$$\mathrm{p_{n,gr}} = \mathrm{mv_{n,gr}} = \frac{\mathrm{Hm}}{\lambda_{n,gr}},$$ eq-19

where H =h/m' is the "quasi-Planck constant", m' is a factor with the unit of mass (kg), m is the mass of the object, see SumQM-2. Then, for the bound state,

$$\mathrm{E_n} = \mathrm{K} + \mathrm{V} = \frac{-1}{2}\mathrm{mv}_{n,gr}{}^2$$ eq-20

$$\mathrm{E_n} = -\mathrm{H}m\mathrm{f_{n,ph}} = -\mathrm{H}m\mathrm{f_{1,ph}}\left(\frac{1}{\mathrm{n}^2}\right)$$ eq-21

Deduced from: $\mathrm{E_n} = \mathrm{K} + \mathrm{V} = \frac{-1}{2}\mathrm{mv}_{n,gr}{}^2 = \frac{-1}{2}\mathrm{p_{n,gr}v}_{n,gr} = \frac{-1}{2}\left(\frac{\mathrm{Hm}}{\lambda_{n,gr}}\right)\left(\frac{2}{n}\mathrm{v_{n,ph}}\right) = \frac{-1}{2}\left(\frac{\mathrm{n}}{\lambda_{n,ph}}\mathrm{Hm}\right)\left(\frac{2}{n}\lambda_{\mathrm{n,ph}}\mathrm{f_{n,ph}}\right) = -\mathrm{H}m\mathrm{f_{n,ph}} = -\mathrm{H}m\mathrm{f_{1,ph}}\left(\frac{1}{\mathrm{n}^2}\right)$

Then, apply above equations to Bohr model's H-atom, we obtained Table 1. It not only fits $\omega_n = v_n / r_n$ perfectly, but also fits the Bohr-de Broglie atom model perfectly (see section III), and also fits the Schrodinger equation/solution perfectly (see section IV). From this work, I am sure that for matter wave, $\mathrm{v_{n,ph}} = \frac{1}{2}\mathrm{v_{n,gr}}$ is also only a special case of the more generalized form $\mathrm{v_{n,ph}} = \frac{\mathrm{n}}{2}\mathrm{v_{n,gr}}$. Therefore, I believed that all QM text books may need to be updated accordingly.

Table 1. Using $\mathrm{v_{n,ph}} = \frac{\mathrm{n}}{2}\mathrm{v_{n,gr}}$ and eq-1 through eq-21 for the calculation of electron and photon (in Bohr model's H-atom).

Bohr model, H-atom					particle E				wave E	transition			Δf_{ph}	photon's Δf	use f_{gr}		photon's Δf		For orbital electron						For photon, $v_{n=2,ph} = v_{n=2,gr}$,			
e-	Z	orbit n =	$r_n = n^2 * r_1/Z$	$v_{n,gr}$=sqrt[e^2*Z/(4π $\varepsilon_0 m r_n$)]	**E_n= -1/2* (1/4πε_0)* Ze^2/r_n**	$\lambda_{n,ph} = 2\pi r_n$	$f_{n,ph} = v_{n,ph}/\lambda_{n,ph} = v_{n,gr}*n/2/(2\pi r_n)$	H=h/m'	**E_n = -Hm $f_{n,ph}$**		$\lambda_{ph,n\to n'}$= c/$f_{n,ph}$ =hc / (E_n- $E_{n'}$)	observed or Ritz $\lambda_{n\to n'}$	$f_{n',ph} - f_{n,ph}$=	$\Delta f_{n,ph}$= c/$\lambda_{ph,n'\to n}$	$f_{n,gr}$= $v_{n,gr}$/ ($2\pi r_n$)	$f_{n,ph}$= $f_{n,gr}$ *n/2 =	$\Delta f_{n,ph}$ = $f_{n',gr}$ *(n'/2) - $f_{n,gr}$ *(n/2) =	$\lambda_{n-n'}$ = c/Δf_{ph}	$\omega_{n,gr}$ = $2\pi f_{n,gr}$= $v_{n,gr}/r_n$	$\omega_{n,ph}$ = $2\pi f_{n,ph}$= $v_{n,ph}/r_n$= (n/2)$v_{n,gr}$ /r_n	$\omega_{n,ph}$ = (n/2) $\omega_{n,gr}$	$\Delta\omega_{n,ph}$ =	angular moment L_n= $m r_n v_{n,gr}$	differ. $\Delta L_n = L_{n+1}$- L_n = h/(2π)	virtual n" correlate to $\Delta f_{n,ph}$ =	$f_{n'',ph}$ = $f_{n'',gr}$ = $\Delta f_{n,ph}$ =	$\lambda_{n'',gr}$ = $\lambda_{n'',ph}$ /2	$\omega_{n'',ph}$ = $2\pi f_{n'',ph}$= $2\pi f_{n'',gr}$
unit			m	m/s	J	m	1/s	J.s/kg	J		nm	nm	1/s	1/s	1/s	1/s	1/s	nm	arc/s	arc/s	arc/s	arc/s	kg*m*m/s	kg*m*m/s		1/s	nm	arc/s
e^-	1	1	5.29E-11	2.19E+06	**-2.18E-18**	3.32E-10	3.29E+15	7.274E-04	**-2.18E-18**						6.58E+15	3.29E+15			4.13E+16	2.07E+16	2.07E+16		1.05E-34	1.055E-34				
e^-	1	2	2.12E-10	1.09E+06	**-5.45E-19**	1.33E-09	8.22E+14	7.274E-04	**-5.45E-19**	$\lambda_{2\to1}$ =	121.50	121.57	2.47E+15	2.47E+15	8.22E+14	8.22E+14	2.47E+15	121.50	5.17E+15	5.17E+15	5.17E+15	-1.55E+16	2.11E-34	1.055E-34	1.387	2.47E+15	60.75	1.55E+16
e^-	1	3	4.76E-10	7.29E+05	**-2.42E-19**	2.99E-09	3.66E+14	7.274E-04	**-2.42E-19**	$\lambda_{3\to1}$ =	102.52	102.57	2.92E+15	2.92E+15	2.44E+14	3.66E+14	2.92E+15	102.52	1.53E+15	2.30E+15	2.30E+15	-1.84E+16	3.16E-34	1.055E-34	1.310	2.92E+15	51.26	1.84E+16
										$\lambda_{3\to2}$ =	656.12	656.28	4.57E+14	4.57E+14			4.57E+14	656.12				-2.87E+15			2.433	4.57E+14	328.06	2.87E+15
e^-	1	4	8.47E-10	5.47E+05	**-1.36E-19**																		4.22E-34					

Note: This table should be used to update SunQM-6s1's Table-1, and also SunQM-2's Table-2.

Table 2. Using $\mathrm{v_{n,ph}} = \frac{\mathrm{n}}{2}\mathrm{v_{n,gr}}$ and eq-1 through eq-21 to update SunQM-2's Table-1 (that is, using E_n = -Hm$f_{n,ph}$ to calculate the planet's orbit energy in Solar system's G-force field, and comparing the results between classical, QM particle, and QM wave calculations).

				classical	QM												
NASA's data of planets				particle E	{N,n} QM model calculated data						particle E_n	wave, set {0,1} as total n=1, calc λ_n, f_n, H, m', E_n,					
	mass	Sun's radius or planet orbit-r	planet orbit-v	**orbit E=-(1/2)mv^2**	{N,n} model , N=	{N,n} model , n=	period factor=	{N,n} model, total n=	{N,n} model $r_n = r_1 n^2$	$v_{n,gr}$ = sqrt(GM/ r_n)	**E_n=-(1/2) $mv_{n,gr}{}^2$**	calc n	$\lambda_{n,ph} = 2\pi r_n$	$f_{n,ph}$= $v_{n,ph}/\lambda_{n,ph}$ =n/2*$v_{n,gr}$ /$\lambda_{n,ph}$	**H= h/m'= 2π*sqrt(GMr_1)**	m'=h/H	**E_n = -Hm $f_{n,ph}$**
unit	kg	m	m/s	J					m	m/s	J		m	1/s	J.s/kg	kg	J
Sun core		1.74E+08			0	1	6	1	1.74E+08	873647		1					
SUN	1.99E+30	6.96E+08			0	2	6	2	6.96E+08	436824		2					
					1	1	6	6	6.26E+09	145608		6					
Mercury	3.30E+23	5.79E+10	47400	**-3.71E+32**	1	3	6	18	5.64E+10	48536	**-3.89E+32**	18	3.54E+11	1.23E-06	**9.55E+14**	6.94E-49	**-3.89E+32**
Venus	4.87E+24	1.08E+11	35000	**-2.98E+33**	1	4	6	24	1.00E+11	36402	**-3.23E+33**	24	6.29E+11	6.94E-07	**9.55E+14**	6.94E-49	**-3.23E+33**
Earth	5.97E+24	1.49E+11	29800	**-2.65E+33**	1	5	6	30	1.57E+11	29122	**-2.53E+33**	30	9.84E+11	4.44E-07	**9.55E+14**	6.94E-49	**-2.53E+33**
Mars	6.42E+23	2.28E+11	24100	**-1.86E+32**	1	6	6	36	2.25E+11	24268	**-1.89E+32**	36	1.42E+12	3.08E-07	**9.55E+14**	6.94E-49	**-1.89E+32**
Jupiter	1.90E+27	7.78E+11	13100	**-1.63E+35**	2	2	5.33	64.0	7.12E+11	13659	**-1.77E+35**	64.0	4.47E+12	9.77E-08	**9.55E+14**	6.94E-49	**-1.77E+35**
Saturn	5.68E+26	1.43E+12	9700	**-2.67E+34**	2	3	5.33	95.9	1.60E+12	9106	**-2.35E+34**	95.9	1.01E+13	4.34E-08	**9.55E+14**	6.94E-49	**-2.35E+34**
Uranus	8.68E+25	2.97E+12	6800	**-2.01E+33**	2	4	5.33	127.9	2.85E+12	6830	**-2.02E+33**	127.9	1.79E+13	2.44E-08	**9.55E+14**	6.94E-49	**-2.02E+33**
Neptune	1.02E+26	4.51E+12	5400	**-1.49E+33**	2	5	5.33	159.9	4.45E+12	5464	**-1.52E+33**	159.9	2.79E+13	1.56E-08	**9.55E+14**	6.94E-49	**-1.52E+33**
Pluto	1.46E+22	5.91E+12	4700	**-1.61E+29**	2	6	5.33	191.9	6.40E+12	4553	**-1.51E+29**	191.9	4.02E+13	1.09E-08	**9.55E+14**	6.94E-49	**-1.51E+29**

NASA's data of planets	wave, set {1,1} as total n=1, calc λ_n, f_n, H, m', E_n,						wave, set {2,1} as total n=1, calc λ_n, f_n, H, m', E_n,						wave, set m'=electron's mass, calc total n=?				
	calc n	$\lambda_{n,ph} = 2\pi r_n$	$f_{n,ph}$= $v_{n,ph}/\lambda_{n,ph}$ =n/2*$v_{n,gr}$ /$\lambda_{n,ph}$	**H= h/m'= 2π*sqrt(GMr_1)**	m'=h/H	**E_n = -Hm $f_{n,ph}$**	calc n	$\lambda_{n,ph} = 2\pi r_n$	$f_{n,ph}$= $v_{n,ph}/\lambda_{n,ph}$ =n/2*$v_{n,gr}$ /$\lambda_{n,ph}$	**H= h/m'= 2π*sqrt(GMr_1)**	m'=h/H	**E_n = -Hm $f_{n,ph}$**	m'= m_e	H=h/m'	$f_{n,ph}$ = -E_n/(Hm)	$\lambda_{n,ph} = 2\pi r_n$	n= $2v_{n,ph}/v_{n,gr}$ =$2\lambda_{n,ph} f_{n,ph}$/ $v_{n,gr}$
unit		m	1/s	J.s/kg	kg	J		m	1/s	J.s/kg	kg	J	kg	J.s/kg	1/s	m	
Sun core	1/6						1/6^2										
SUN	2/6						2/6^2										
	1						1/6										
Mercury	3	3.54E+11	2.06E-07	**5.73E+15**	1.16E-49	**-3.89E+32**	3/6	3.54E+11	3.43E-08	**3.44E+16**	1.93E-50	**-3.89E+32**	9.11E-31	7.27E-04	1.62E+12	3.54E+11	2.36E+19
Venus	4	6.29E+11	1.16E-07	**5.73E+15**	1.16E-49	**-3.23E+33**	4/6	6.29E+11	1.93E-08	**3.44E+16**	1.93E-50	**-3.23E+33**	9.11E-31	7.27E-04	9.11E+11	6.29E+11	3.15E+19
Earth	5	9.84E+11	7.40E-08	**5.73E+15**	1.16E-49	**-2.53E+33**	5/6	9.84E+11	1.23E-08	**3.44E+16**	1.93E-50	**-2.53E+33**	9.11E-31	7.27E-04	5.83E+11	9.84E+11	3.94E+19
Mars	6	1.42E+12	5.14E-08	**5.73E+15**	1.16E-49	**-1.89E+32**	1	1.42E+12	8.57E-09	**3.44E+16**	1.93E-50	**-1.89E+32**	9.11E-31	7.27E-04	4.05E+11	1.42E+12	4.73E+19
Jupiter	10.7	4.47E+12	1.63E-08	**5.73E+15**	1.16E-49	**-1.77E+35**	1.8	4.47E+12	2.71E-09	**3.44E+16**	1.93E-50	**-1.77E+35**	9.11E-31	7.27E-04	1.28E+11	4.47E+12	8.39E+19
Saturn	16.0	1.01E+13	7.24E-09	**5.73E+15**	1.16E-49	**-2.35E+34**	2.7	1.01E+13	1.21E-09	**3.44E+16**	1.93E-50	**-2.35E+34**	9.11E-31	7.27E-04	5.70E+10	1.01E+13	1.26E+20
Uranus	21.3	1.79E+13	4.07E-09	**5.73E+15**	1.16E-49	**-2.02E+33**	3.6	1.79E+13	6.79E-10	**3.44E+16**	1.93E-50	**-2.02E+33**	9.11E-31	7.27E-04	3.21E+10	1.79E+13	1.68E+20
Neptune	26.7	2.79E+13	2.61E-09	**5.73E+15**	1.16E-49	**-1.52E+33**	4.4	2.79E+13	4.34E-10	**3.44E+16**	1.93E-50	**-1.52E+33**	9.11E-31	7.27E-04	2.05E+10	2.79E+13	2.10E+20
Pluto	32.0	4.02E+13	1.81E-09	**5.73E+15**	1.16E-49	**-1.51E+29**	5.3	4.02E+13	3.02E-10	**3.44E+16**	1.93E-50	**-1.51E+29**	9.11E-31	7.27E-04	1.42E+10	4.02E+13	2.52E+20

(Note: The key difference between the two results was that, while $\mathrm{v_{n,ph}} = \frac{1}{2}\mathrm{v_{n,gr}}$ produced $\lambda_{\mathrm{n,ph}} = n\lambda_{\mathrm{1,ph}}$ (in SunQM-6s1's eq-9 & eq-10), the new $\mathrm{v_{n,ph}} = \frac{\mathrm{n}}{2}\mathrm{v_{n,gr}}$ produced $\lambda_{\mathrm{n,ph}} = n^2\lambda_{\mathrm{1,ph}}$ (see eq-8). As shown in section III and section IV, it is this n^2 that gives the key physical meaning of the phase wave in the matter wave).

(Note: Under {N,n} QM, eq-1 through eq-21 should work for both micro-world and macro-world (see Table 1 and Table 2). For Bohr model's particle mechanics, we should use eq-20 and the related group velocity for the calculation, and the $\lambda_{n,gr}$ and $f_{n,gr}$ is not much useful; For Bohr model's wave mechanics, we should use eq-21 and the related phase wave parameters for the calculation. Similarly, for macro-world's particle mechanics, we should use eq-20 and the related group velocity for the calculation, and the $\lambda_{n,gr}$ and $f_{n,gr}$ is not much useful; For macro world's wave mechanics, we should use eq-21 and the related phase wave parameters for the calculation).

(Note: For Bohr atom's particle description version and/or (de Broglie) matter wave description version, see Appendix A for the updated SunQM-6s1's eq-1 through eq-20). (Note: For the same reason, the deduction of SunQM-4's eq-19 through eq-41 should also be re-do accordingly by using $v_{n,ph} = \frac{n}{2} v_{n,gr}$, (rather than $v_{n,ph} = \frac{1}{2} v_{n,gr}$), see Appendix B for details).

According to wiki "Matter wave (2023/09/22 version)", "*Electromagnetic waves also obey* $\boldsymbol{v_p} * \boldsymbol{v_g} = c^2$ *, as both* $|\boldsymbol{v_p}| = c$ *and* $|\boldsymbol{v_g}| = c$". Then for a photon, we can use eq-1 through eq-21 with n = 2 to describe:

$v_{n,ph} = \frac{n}{2} v_{n,gr}$ (eq-1) $\rightarrow v_{2,ph} = v_{2,gr}$, or $\mathbf{v_{phot,ph} = v_{phot,gr} = c}$, eq-22-photon

$\lambda_{n,ph} = n\lambda_{n,gr}$ (eq-11) $\rightarrow \lambda_{2,ph} = 2\lambda_{2,gr}$, or, $\boldsymbol{\lambda_{phot,ph} = 2\lambda_{phot,gr}}$, eq-23-photon

$f_{n,ph} = \frac{n}{2} f_{n,gr}$ (eq-14) $\rightarrow \mathbf{f_{phot,ph} = f_{phot,gr}}$, eq-24-photon

Thus, using $v_{n,gr} = n\lambda_{n,gr} f_{n,gr}$ (eq-3) and $v_{n,ph} = \lambda_{n,ph} f_{n,ph}$ (eq-10), we have

$v_{n=2,ph} = \lambda_{n=2,ph} f_{n=2,ph} = c = v_{n=2,gr} = 2\lambda_{n=2,gr} f_{n=2,gr}$, eq-25-photon

and everything fit well. Then, according the eq-10, $v_{n,ph} = \lambda_{n,ph} f_{n,ph} = c$, **the base wavelength of a photon (that we used every day) must be the phase wavelength**! Then, a photon's (unused) group wavelength is half of the commonly used (phase) wavelength (see Table 1 columns 25 ~ 26).

(Note: In SunQM-6's section-V, a photon was also assigned to have a fixed n = 2 QM state for the explanation of the propagation).

II. Re-explain the difference between Bohr model (of 1D-circular QM) and a general 1D-circular QM model

In SunQM-4s1's Fig-2 and Fig-3, I explained the difference between Bohr model (of 1D-circular QM) and a general model of 1D-circular QM. Now I need to re-explain it with some minor modifications: while Bohr model (of 1D-circular QM) is always limited to n = j, a general model of 1D-circular QM can have j = ½, 1, 3/2, 2, 5/2, 3, 7/2, 4, … etc. for each of any n orbit (see Figure 1 and Figure 4 for more detailed explanations). For example, for Earth's orbit in the Solar system {1,5//6} = {0,30//6}, we can use Bohr model with n = j = 5, or n = j = 30 to describe this orbit; we also can use a general 1D-circular QM model with n = 5 and j =1, or even with n = 1 and j =1, or even with n = 1 and j =1/2 to describe this single orbit that has a single planet in it, (and with the sacrifice that all other planets' quantum numbers have been messed up).

III. de Broglie wave in the Bohr atom model may have already included the paired (up/down) spin information of the electrons

First, let me explain one simplest case. All text books showed us that in any (atomic number) Z > 1 atom's ground state n=1 orbit, there are always two electrons (one spin-up and one spin-down). Here we can use n=1 and j=1 QM state (see

in Figure 1a) to describe them. Because in n=1 orbit it has to have one complete wave (i.e., the rule of de Broglie wave), and one complete wave always contains one positive peak and one negative peak (see in Figure 1a, the j=1 wave in grey line). In Born probability density, this pair of positive/negative peaks becomes two positive probability peaks (see in Figure 1a, the j=1 wave in black line), and these two Born probability peaks represents the two electrons in the n=1 orbit (as explained in all QM text books). Now, if we use the NBP (that directly equals to the wave function (see SunQM-4 and SunQM-4s1), or directly equals to the matter wave, i.e., grey line wave in Figure 1a the j=1 wave), and then let's define that the positive peak represents the spin-up ↑ electron, and the negative peak t represents the spin-down ↓ electron, and then, this NBP density's positive/negative peak pair (or, a pair of positive/negative peak in one de Broglie wave) represents a pair of spin ↑↓ electrons. Then, for all other n ≥ 2 orbits (of any Z > 1 atom's ground state), the de Broglie matter wave in a Bohr atom orbit always has the integer number of the complete wave in φ-1D. That means it always has an integer number of pairs of positive/negative peaks, thus the integer number of pairs ↑↓ electrons. Therefore, using Figure 1, I explained why the de Broglie wave in the Bohr atom model already includes the paired (up/down) spin information.

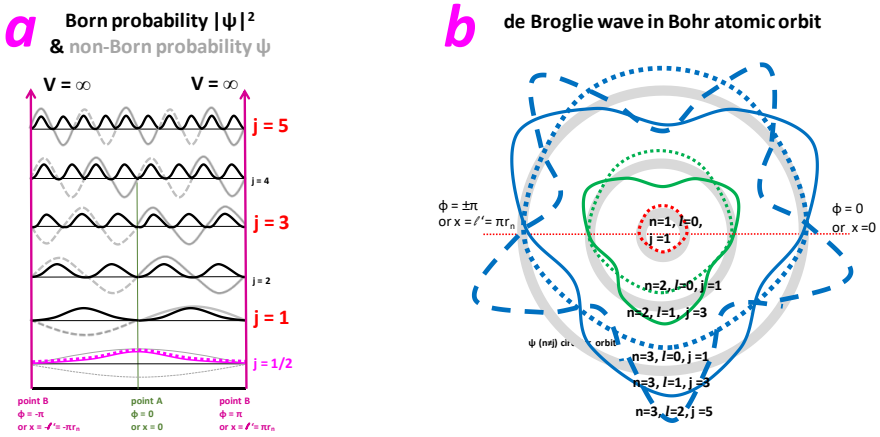

Figure 1a. The Born probability (BP) and the non-Born probability (NBP) in a 1D infinitely deep potential well (that equals to the 1D-circular QM's potential well). Copied and modified from SunQM-4s1's Fig-3d.
Figure 1b. de Broglie wave in Bohr atomic orbit, represented by the NBP, and in phase wave (so that each positive/negative wave peak represents a pair of spin up-down electrons). Copied and modified from SunQM-4s1's Fig-2b.

Table 3. Pair number of spin ↑↓ electrons in each n orbit.

orbit n =	n^2=	ground state electron configuration in each n orbit	electron pair number in each n orbit	electron number in each n orbit	n orbit shell volume = 4/3*π* (r_{n+1}^3-r_n^3)	electron density per n orbit shell volume
1	1	$1s^2$	1	2	263.9	0.00758
2	4	$2s^2 2s^6$	4	8	2785.5	0.00287
3	9	$3s^2 3s^6 3d^{10}$	9	18	14103.7	0.00128
4	16	$4s^2 4s^6 4d^{10} 4f^{14}$	16	32	48292.6	0.00066
5	25	$5s^2 5s^6 5d^{10} 5f^{14} 5g^{18}$	25	50	129982.3	0.00038
6	36	$6s^2 6s^6 6d^{10} 6f^{14} 6g^{18} 6h^{22}$	36	72	297374.8	0.00024
7	49	$7s^2 7s^6 7d^{10} 7f^{14} 7g^{18} 7h^{22} 7i^{26}$	49	98		

After digging more, I found that the pair number of electrons in each n orbit (of Bohr-like atom model) is directly correlated to the phase wavelength's formula of $\lambda_{n,ph} = n^2\lambda_{1,ph} = 2\pi r_1 n^2$ (eq-8). In this formula, if we treat each $2\pi r_1 = \lambda_{1,ph}$ (i.e., one complete phase wave at n=1 orbit) contains one pair of spin ↑↓ electrons, then, as shown in the calculation in

Table 3, at orbits of n=1, 2, 3, 4, 5, 6, 7, eq-8 predicted that there are n^2 number (i.e., 1, 4, 9, 16, 25, 36, 49) pairs of electrons in each n orbit. These pair numbers (in column 2) are perfectly matched to the number given from QM text books (see in column 3 and column 4 of Table 3).

After further digging, I further found that the phase wavelength formula eq-8 is able to explain not only the electron number in each n shell orbit, but also the electron number in each *l* sub-shell orbit. See in Figure 1b, for n=1 orbit, it should be described by n=1 and j=1 QM state, with one pair of positive/negative NBP peak and thus one pair of spin ↑↓ electrons; Then, for n=3 shell orbit's *l*=0 ($3s^2$) sub-shell, it should be described by n=3 and j=1 QM state, with one pair of positive/negative NBP peak and thus one pair of spin ↑↓ electrons; for n=3 shell orbit's *l*=1 ($3p^6$) sub-shell, it should be described by n=3 and j=3 QM state, with three pair of positive/negative NBP peaks and thus three pair of spin ↑↓ electrons; for n=3 shell orbit's *l*=2 ($3d^{10}$) sub-shell, it should be described by n=3 and j=5 QM state, with five pair of positive/negative NBP peaks and thus five pair of spin ↑↓ electrons; and so on so forth.

Furthermore, it seems that the de Broglie wave description for each n orbit can be used for either the group wave or the phase wave. For example, for n=1 orbit, it has circumference of $2\pi r_1$; for the n=3 orbit, it has circumference of $2\pi r_n = 2\pi r_1 n^2 = 18\times(2\pi r_1)$, under the electron ground state with 100% electron occupancy, it correlates to 18 electrons ($3s^2 3p^6 3d^{10}$, or 9 pairs of ↑↓):

1) If using phase wave to represent, then eq-8 ($\lambda_{n=3,ph} = 2\pi r_1 n^2$) directly presents 9 pairs of electron (total =18 electrons). So, the physical meaning of the phase wave is that it correlates to the pair number of electrons (that paired as spin ↑↓) in the n orbit;
2) If using group wave to represent, then eq-6 ($\lambda_{n=3,gr} = 3 \times 2\pi r_1 = 3 \times \lambda_{1,gr}$) has the physical meaning of, the n=3 orbit contains three de Broglie waves (this is the original definition of de Broglie wave in Bohr orbit, see [33]), and each n=3 de Broglie wave has a length at 3 times of the length at n=1's de Broglie wave.
3) This means, it is the phase wave that reflects each single electron/object's true matter wave property, the group wave only reflects the property of all electrons/objects as a group.

IV. Schrodinger equation/solution (in form of the non-Born probability) may also already include the paired (up/down) spin information of the electrons

Because all electrons in n=3 θφ-2D space must be in RF (RotaFusion, or rotation diffusion) mode, under a snap-shot, all electrons in n=3 θφ-2D space must be (roughly) evenly distributed in the n=3 θφ-2D space. Based on this idea, I constructed Figure 2, in which Re[Y(*l'*,m')] is chosen to be *m'* = n = 1, 2, 3, 4, 5, 6, 7,
Re[Y(*l'*=1,*m'*=1)] has one pair of positive/negative peak, equals to n=1 orbit shell, or $1s^2$ electrons, see Figure 2a;
Re[Y(*l'*=3,*m'*=2)] has total 4 pairs of positive/negative peak, 2 pairs per layer and there are 2 layers totally, equals to n=2 orbit shell, or $2s^2 2s^6$ electrons, see Figure 2b;
Re[Y(*l'*=5,*m'*=3)] has total 9 pairs, 3 pairs per layer, and 3 layers total, equals to n=3 orbit shell, $3s^2 3s^6 3d^{10}$, see Figure 2c;
Re[Y(*l'*=7,*m'*=4)] has total 16 pairs, 4 pairs per layer, 4 layers total, equals to n=4 orbit shell, $4s^2 4s^6 4d^{10} 4f^{14}$, see Figure 2d;
Re[Y(*l'*=9,*m'*=5)] has total 25 pairs, 5 pairs per layer, 5 layers total, see Figure 2e;
Re[Y(*l'*=11,*m'*=6)] has total 36 pairs, 6 pairs per layer, 6 layers total, see Figure 2f;
Re[Y(*l'*=13,*m'*=7)] has total 49 pairs, 7 pairs per layer, 7 layers total, see Figure 2g;
Thus, *m'* means how many pair of electrons per φ-1D space (per one layer in θ-1D); and (*l'* – *m'*+1) means how many layers in θ-1D space. (Note: the *l* = 0, 1, 2, … in the normal Re[Y(*l*,m)] seems do not have any direct meaning in Figure 2). After adding Im[Y(*l'*,*m'*)], it makes those positive/negative peaks to rotate around z axis.

While Figure 1b is able to present electrons in each *l* sub-shell (that within one n orbital shell, but only presented in φ-1D space), Figure 2 can only present all electrons (within one n orbital shell) on one θφ-2D spherical surface, (that is, all electrons in all *l* sub-shells have to be merged onto a single spherical surface), it does not provide any information on the electron pairs in each *l* sub-shell. However, we may can force it to add this information by using our imagination: for example, in the n=3 shell, for the repulsive force within θφ-2D space (like the electrons in an atom), you can imagine that in

Figure 2c, one pair of positive/negative peak is a little bit below the spherical surface, three pair of positive/negative peaks are at exactly the spherical surface, and the rest five pair of positive/negative peaks are at a little bit outside of the spherical surface (Note: this should be allowed, because 3s, 3p, 3d sub-shells do overlap mostly in the r-1D space, see SunQM-6s4's Fig-1a). Of cause, you need to make these two, six, and ten electrons roughly evenly distributed in each own *l* sub-shell's θφ-2D space.

Therefore, the phase wavelength formula of $\lambda_{n,ph} = n^2\lambda_{1,ph} = 2\pi r_1 n^2$ (eq-8) has different meaning in Figure 2 than in Figure 1b. In Figure 2, it means that there are n phase waves in (one layer of) φ-1D space and n layers in θ-1D space, so it formed n × n = n^2 of phase waves in the θφ-2D space; while in Figure 1b, it means that there are total n^2 phase waves in φ-1D space (if all *l* sub-shells are merged into one). Again this means, it is the phase wave that reflects each single electron/object's true matter wave property, the group wave only reflects the property of all electrons/objects as a group.

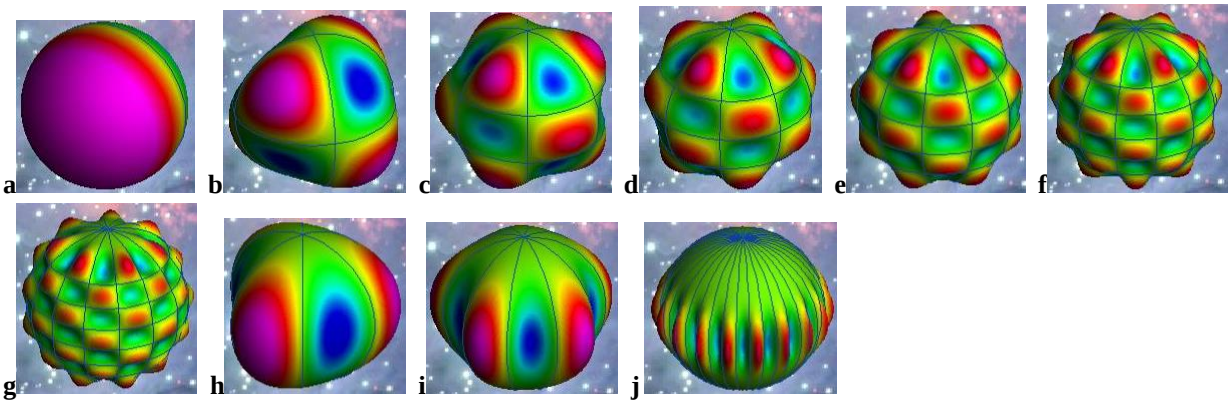

Figure 2 (a, b, c, d, e, f, g, h, i, and j). Spherical surface (or solid) plot of Re[Y(*l'*=1,*m'*=1)], Re[Y(*l'*=3,*m'*=2)], Re[Y(*l'*=5,*m'*=3)], Re[Y(*l'*=7,*m'*=4)], Re[Y(*l'*=9,*m'*=5)], Re[Y(*l'*=11,*m'*=6)], Re[Y(*l'*=13,*m'*=7)], Re[Y(*l'*=3,*m'*=3)], Re[Y(*l'*=5,*m'*=5)] , and Re[Y(*l'*=18,*m'*=18)]. Plotted by using the (free) online plotter at "http://icgem.gfz-potsdam.de/vis3d/tutorial".

Can we use θφ-2D wave function (or NBP) to present Figure 1b? I tried, the answer is "No". For example, for n=3, if using Re[Y(*l'*,*m'*)], we can only use nLL mode (such as Re[Y(*l'*=1,*m'*=1)], Re[Y(*l'*=3,*m'*=3)], Re[Y(*l'*=5,*m'*=5)], Re[Y(*l'*=18,*m'*=18)], shown in Figure 2 (a, h, i, j)) to present. (Note: For Re[Y(*l'*,*m'*)] in nLL mode, *l'* = *m'* = j). Obviously, electrons are impossible to distribute in the n=3 θφ-2D space in this way. Only the normal Re[Y(*l*,*m*)] with *l* =0, 1, 2, 3 … can represent s, p, d, f … sub-shell within each n shell. Then, why the *l* in the normal R(*n*,*l*) is different than the *l'* in Re[Y(*l*',*m'*)] ? The answer is: because the Re[Y(*l*',*m'*)] only presents the all *l* sub-shells merged wave function, so its *l*' does not correlate anymore to the *l* =0, 1, 2, 3, or s, p, d, f sub-shell within each n shell.

Then, how to explain that, for n=2, there are |2,0,0>, |2,1, m=0,±1>, total 4 states; For n=3, there are |3,0,0>, |3,1, m=0,±1>, |3,2, m=0,±1,±2>, total 9 states; For n=4, there are |4,0,0> , |4,1,m=0,±1> , |4,2,m=0,±1,±2> , |4,3,m=0,±1,±2,±3> , total 16 states? Remember each state contain two electrons (spin ↑↓). This description is exactly same as the description of $1s^2 2s^2 2p^6 3s^2 3p^6 3d^{10}$. The answer is, all these QM states were obtained from the Schrodinger equation/solution. As shown in Griffiths book p152, eq-4.85, for each n shell (or state), there are *l* = 0, 1, 2, … n-1 sub-shells (or sub-states); and for each *l* sub-shell, there are m = 2*l*+1 sub-states. So, the total degeneracy of the energy level E_n is

$$d(n) = \sum_{l=0}^{n-1}(2l+1) = n^2 \qquad \text{eq-26 (Griffiths' eq-4.85)}$$

After all, the physical meaning of the phase wavelength formula of $\lambda_{n,ph} = n^2\lambda_{1,ph} = 2\pi r_1 n^2$ (eq-8) is directly come from eq-26. Therefore, this may be a new way to use NBP (or the Re[Y(*l'*,m')] wave function) to present the electron (including the spin state) distribution in each n shell.

The next question is, because in the {N,n} QM, the Schrodinger equation/solution (in forms of NBP) does contain the paired up/down spin information of two electrons, will it do the function of the Pauli spin matrices (see Griffiths' p174 eq-4.148)?

V. Schrodinger equation's solution (in BP or NBP density) may already show that the fermion density has a spherical multiple shell-like structure that equivalent to the 3D wave packet

Column 3 of Table 3 showed the electron number per each *l* sub-shell. (Notice that this number was obtained from Schrodinger equation/solution). In column 6 of Table 3, the shell volume of each n orbital shell was calculated (by assuming $r_1 = 1$, $r_n = r_1\, n^2 = n^2$, and $V_{n+1} - V_n = (4/3)\pi(r_{n+1}^3 - r_n^3) = (4/3)\pi\{[(n+1)^2]^3 - [(n)^2]^3\} = (4/3)\pi[(n+1)^6 - n^6]$). In column 7, the electron density per each n orbital shell was estimated (based on the rule of "all mass between r_n and r_{n+1} belongs to orbit n (see paper SunQM-3s2)"). Figure 3a illustrated the electron density (at an arbitrary scale) that not only based on the n shells, but also based on the (estimated) *l* sub-shells. (Note: From the previous result of the repulsive force in θφ-2D space (see SunQM-6s6), here I assumed that within each n shell, the higher the *l*, the higher the electron density. Notice that this is a citizen scientist leveled assumption). In Figure 3b, I replaced the electrons with the general fermions that have the attractive force in θφ-2D space (just like the mass in a pre-Sun ball), and then showed the fermion density (or mass density) not only based on the n shells, but also based on the (estimated) *l* sub-shells. (Note: I assumed that there are same number of fermions per each *l* sub-shell in both Figure 3b and Figure 3a, and this is a citizen scientist leveled assumption). (Note: From the basic physical knowledge, the attractive force in θφ-2D space must cause that the inner the *l* sub-shell, the higher the fermion density, as shown in Figure 3b. Then, using the result obtained in SunQM-6s6's section III, the inner the *l* sub-shell under the attractive force will have higher *l* number, as shown in Figure 3b).

In both Figure 3a and Figure 3b, we see that besides the major r-1D E-force (or r-1D G-force) caused electron density major decreasing (see the red dotted-line), there is a minor θφ-2D E-force (or θφ-2D G-force) caused density ripples in r-1D (see the red solid wave-line in Figure 3). Combining these two curves produces a stepped-downward (r-1D density) curve as shown in SunQM-6s4's Fig-1b curve of "Σ(n=1..5)". This means that for fermions (note: both electron and the matter in the pre-Sun ball are all belong to fermion), Schrodinger equation's solution (in Born probability density) already produced that the fermion density has a spherical multi-shell like structure (based on each n shell, for all n shells), so that we can see clearly the onion-like shell structure (based only on the fermion density). For the repulsive force in θφ-2D space, the highest fermion density (i.e., the electron density) may be close to the outer-edge of each n shell (see Figure 3a); while for the attractive force in θφ-2D space, the highest fermion density (or the pre-Sun's mass density) may be close to the inner-edge of each n shell (see Figure 3b). This makes sense (according to the basic physics): the repulsive electrons (in the same n shell) makes them concentrated at the outer edge of the n shell, and the attractive matter (in the same n shell) makes them concentrated at the inner edge of the n shell.

This (n-shell based) fermion density shell structure also correlates well with the 3D wave packet description (that is also a n-shell based NBP or BP density shell structure). So now we see that the 3D wave packet is not only a mathematical model for the description of {N,n} QM structure, but it also may have been supported by the real physical structure that based on the fermion density.

Thus, this analysis again showed that, the quantum phenomenon is produced by the interference of the 3D spherical wave of a point-centered field (of force, mass, energy, etc.) to become a spherical 3D wave packet, so that the NBP (= wave) peaks at some positions and valleys at some other positions, (also see SunQM-2's section IV for the similar description).

If this is correct, then (from Figure 3b) we can further predict that the (fermion) mass density of the residue |n,L,L> QM state (stream-like) mass (that under the attractive force in θφ-2D space) may should have a little bit higher mass density than the surrounding |(n-1),0,0> QM state mass. For example,

1) As shown in SunQM-3s3's Fig-4, on the Jupiter surface, the (stream-like) zonal bands |5,4,m> may have mass density higher than the surrounding |4,0,0> QM state belt band mass;

2) As shown in SunQM-4s2's Fig-3, in the Earth atmosphere, the (stream-like) polar jet (that may be the effective |3,2,0> QM state) and the subtropical jet (that may be the effective |3,2,1> QM state) may have mass density higher than the surrounding tropopause layer mass (that may be the effective |2,0,0> QM state);
3) As shown in SunQM-3s9's Fig-10, in the Earth mantle layer's outer edge, the residue |2,1,1> (then to |4,3,3>, then to higher n of |n,L,L>) mode stream-like mass (that in phase-1) may have mass density higher than the surrounding mantle layer mass (that may be the effective |1,0,0> QM state);
4) As shown in SunQM-3s9's Fig-1, in the Sun surface layer, the residue |2,1,1> (then to |4,3,3>, then to higher n of |n,L,L>) mode stream-like mass (that in phase-1) may have mass density higher than the surrounding mass (that may be in the effective |1,0,0> QM state).

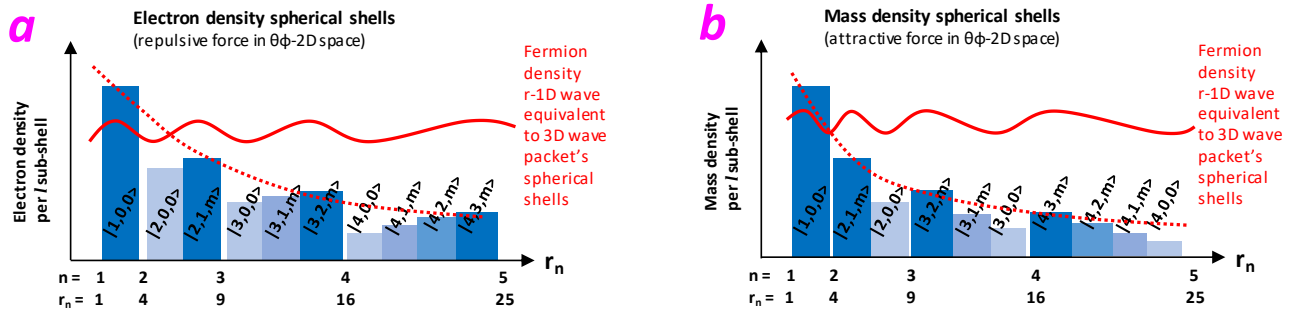

Figure 3a. Qualitatively estimated electron density per each n shell, and per each *l* sub-shell (under the repulsive θφ-2D force). Note: y-axis is in arbitrary scale.
Figure 3b. Qualitatively estimated fermion density per each n shell, and per each *l* sub-shell (under the attractive θφ-2D force).

VI. "Mobius strip" effect may can be explained by using the general 1D-circular QM with the half integer j =1/2, 3/2, etc. and $\mathbf{v_{n,ph}} = \frac{\mathbf{n}}{2}\mathbf{v_{n,gr}}$

So far I have explained three different ways to present the same (bound state orbital moving) NBP density peaks. The first way is either directly using the 1D-circular QM's de Broglie wave (see section III), or directly using Schrodinger equation's solution to present the NBP density (positive/negative) peaks (see section IV that using Y(*l',m'*)). Although the first way is the simplest way, it has an obvious limitation: it can only be used to present even number of electrons (or objects) per n orbit with the physical property that can be correlated to the positive/negative peak of the NBP density (like spin up-down for electrons). It can't be used to present the odd number of electron per n orbit (or, a planet Earth in the orbit of {1,5} in Solar system). (Note: This result also explains why all Z = even number atoms have higher abundancy (= high stability) than their neighboring Z = odd number atoms (see in SunQM-5's Fig-2), it is because every Z = even number nucleus contains a integer number (= Z/2) of electron pair, so these nucleus are in the comfortable state and have the relative high nuclear stability (relative to the Z = odd number nucleus).

The second way also uses de Broglie wave in 1D-circular QM and/or uses Y(*l*,*m*) in the Schrodinger QM, but indirectly: it needs to "*to lift-up wave function by one to make its min =0, and then divided by two to make its max =1, so its NBP = [1 + cos(x)]/2*", see SunQM-4s1. A more generalized model is shown in SunQM-4s1's Fig-2b, in which for any n orbit, there are j = 1, j = 2, j = 3, ... of de Broglie waves can be used to present one, or two, or three NBP in this n orbit (see SunQM-4's Fig-4c). The advantage of doing this is now we can use it to present either odd or even number particle/planet in a single n orbit (or n shell). For example, a planet Earth in the orbit of {1,5} in Solar system now can be presented in this way (notice that it doesn't has the "Mobius strip" effect). Another example: In SunQM-4s2's Fig-8b, I treated the positive peak of

Y(l,m) as the baseline, then the negative peaks can be used to present the low (air) mass density centers (that eventually forms an extreme quantum weather). (Note: In SunQM-4s2, I used Y(l,m), and it is different than the Y(l',m') in section IV).

The third way is specifically used for a single object moving in the n=1 orbit (or any n orbit) that appeared to have the "Mobius strip" effect in its physical property. In this case, instead of using Figure 1, we have to use the more generalized 1D-circular QM model (that is mentioned in section II): as shown in Figure 4a, for each n orbit in the 1D-circular QM, there are j = ½, 1, 3/2, 2, 5/2, 3, 7/2, 4, … de Broglie waves that are possible to exist in this n orbit. For j equals the integer number, the result is the same as in Figure 1, and there is no Mobius strip effect. For j equals to the half integers (likes ½, 3/2, 5/2, etc.), all of them showed up the Mobius strip effect: one circular orbital movement (360°) does not return to the original QM state, it needs two circular movement (720°) to return to the original QM state (see Figure 4c). For example, in Figure 4a (and Figure 4b) in the j = ½ mode, a circular movement of φ = 0° → 180° → 360° (following the red arrows) causes the QM state from the positive peak of NBP to the negative peak of NBP, then, after the second circular movement of φ = 360° → 720° (following the green arrows), the QM state will return to the original positive peak of NBP. In the same way, we can use Figure 4a to explain "high order Mobius strip" at j = 3/2, 5/2, etc.

Using eq-1, $v_{n,ph} = \frac{n}{2} v_{n,gr}$ (and/or $\omega_{n,ph} = \frac{n}{2} \omega_{n,gr}$), we may can explain the physical meaning of the "Mobius strip" effect. At n=1, $v_{1,ph} = \frac{1}{2} v_{1,gr}$ means phase velocity is only half of the group velocity, so that when the object (that correspond to $v_{1,gr}$) moved 360°, its phase wave only moved 180°, and after the object moved 720°, its phase wave finishes 360°. (Note: According to the result from section III and IV, it is the phase wave that reflects each single electron/object's true matter wave property, the group wave only reflects the property of all electrons/objects as a group. So we need to wait for the phase wave to finish the whole wave before we can say the whole process is finished). (Note: See the alternative explanation in Figure 5c, in which a single electron's phase wave moved 360° while the group electrons only moved 180°). For the high order Mobius strip at j = 3/2, we may can explain it as: at n=3, $v_{3,ph} = \frac{3}{2} v_{3,gr}$ means phase velocity is 1.5x of the group velocity, so that when the object (that correspond to $v_{1,gr}$) moved 360°, its phase wave overshot to 1.5×360°, and after the object moved 720°, its phase wave finishes 3×360°, and it needs the both the group wave and the phase wave to finish integer number rounds to return to the original QM state. I hope that Figure 4 can be helpful in explaining Robert Boyd's result [34] on the "Möbius strips of polarization having 3/2 or 5/2 twists".

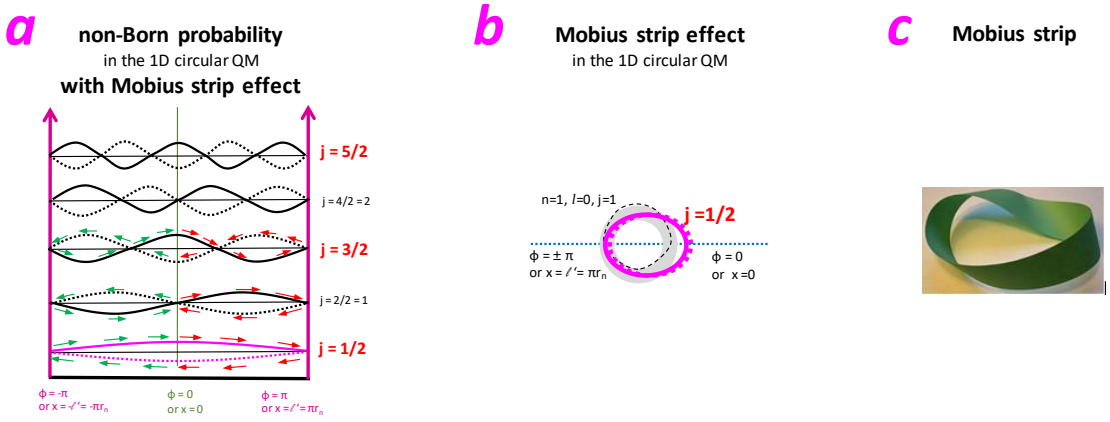

Figure 4a. The non-Born probability (NBP) in a 1D infinitely deep potential well (that equals to the 1D-circular QM's potential well), including the half integer j. Copied and modified from SunQM-4s1's Fig-3d.
Figure 4b. Illustration of the Mobius strip effect in the 1D-circular QM with n=1 and j= ½.
Figure 4c. A Mobius strip.

Thus, the wave function (or NBP) is only a general mathematic description, and it can be further explained in different ways in physics (as needed): 1) In the case of describing one pair or many pairs of spin ↑↓ electrons in one n orbit,

we can choose the NBP to be directly equals to the wave function, so that the positive/negative wave peak is used to represent the paired spin ↑↓ electrons; 2) In the case of describing only a single planet in single one n orbit, I used SunQM-4's eq-10 (or SunQM-4s1's eq-26) to transform the wave function's positive/negative wave peaks into the positive-only probability density peak.

Here are the more examples that the NBP can be used differently for different purpose: First, for the Schrodinger equation's θφ-2D solution Y(*l*,*m*), we can use NBP to represent either the air mass density, or the air pressure, or the air temperature (see more explanation in SunQM-4s2); Second, in SunQM-6s4's eq-2, NBP can be used to fit for a point charge's either static electric field E ∝ 1/r^2 curve, or the potential field U ∝ 1/r curve.

VII. A possible origin of the electron's spin and the nucleon's spin

According to all the QM text books, the origin of the electron's spin is unclear. In this section, I proposed a possible origin of the electron spin and the nucleon spin in an atom. (Note: All work in this section belongs to a citizen scientist leveled work, because it completely violates the mainstream's spin theory).

VII-a. Hypothesis: the face-to-face tidal-locked state is the Eigen state (or the global energy minimum state) of a binary orbital movement.

In SunQM-6s2's Appendix-B, I had guessed that "... *In the case of H-atom… the $\vec{E}$ vector is formed from proton to electron, and the rotation of the $\vec{E}$ is caused by the orbital moving of electron around the proton. ... in a H-atom, both the proton and the electron are always face-to-face tidal-locked, and both are doing anti-clock orbital motion around their reduced mass center ...*".

In the macro world, the Pluton-Chiron binary is the most iconic example of the face-to-face tidal-locked binary orbital motion (see wiki "Pluto"). However, more often we see only the "slave" celestial body is doing the face-tidal-locked binary orbital rotation around the "master" celestial body. For example, the Moon (the "slave") is doing the exact face-tidal-locked binary orbital rotation around the Earth (the "master"), and both Venus (with a day of -5832 hours, the "slave") and Mercury (with a day of 1407 hours, the "slave") are doing (nearly) the face-tidal-locked binary orbital rotation around the Sun (the "master"). It looks like the stronger the attractive force, the more chance that the "slave" object will do the face-tidal-locked binary orbital rotation around the "master" object If the "slave" object has the comparable mass as that of the "master" object, then (without the external disturbance), the strong attractive force will eventually make the two objects to do the face-to-face tidal-locked binary orbital rotation (like the Pluton-Chiron pair does). (Note: I guess that this must have been proved in the classical physics over 100 years ago. If readers know, please tell me). From this analysis, I hypothesized that for the G/RFg-forced binary orbital movement, the face-to-face tidal-locked configuration is the global energy-minimum configuration.

VII-b. Hypothesis: The origin of the electron spin may come from the face-to-face tidal-locked binary orbital motion between an electron and a nuclear proton (using H-atom as the example), and it perfectly fits to the "proton-electron mirror-coupled orbit" model

Similarly, for the E/RFe-forced binary orbital motion, I hypothesized that the face-to-face tidal-locked configuration is also the global energy-minimum configuration (or, the default configuration). It is named here as the "**face-to-face tidal-**

locked binary" model. This hypothesis also perfectly fits to the new "proton-electron mirror-coupled orbit" model (see SunQM-6s6's section IV-b).

Now let's apply this hypothesis to the H-atom. When the proton-electron pair is face-to-face tidal-locked, while doing the binary mutual orbital movement, both proton and electron have to do the spin movement with the same spin-speed (Note: Here the **spin-speed** is defined as the angular velocity/frequency ω_{spin}), and this spin-speed ω_{spin} must equals to the electron's orbital angular velocity $\omega_{orbit,elec}$. So, for both electron and proton (in an H-atom), its spin speed $\omega_{spin,elec} = \omega_{spin,prot} = \omega_{orbit,elec}$. Figure 5a showed a single electron is doing orbital rotation in an H-atom (with its spin face-to-face locked to proton's spin).

Based on this hypothesis, column 21 of Table 1 showed that an n=3 electron (in an H-atom) should have spin speed $\omega_{n=3,ph} = 2\pi v_{n=3,ph}/r_{n=3}$ = 2.30E+15 arc/s, an n=2 electron should have spin $\omega_{n=2,ph} = 2\pi v_{n=2,ph}/r_{n=2}$ = 5.17E+15 arc/s, and an n=1 electron should have spin $\omega_{n=1,ph} = 2\pi v_{n=1,ph}/r_{n=1}$ = 2.07E+16 arc/s. Then, an electron transition from n=3 to n=2 should produce a difference of the electron spin $\omega_{n=2,ph} - \omega_{n=3,ph}$ = 2.87E+15 arc/s (see column 23), and, according to for the conservation of spin angular momentum, this difference should be carried away by the emitted 656.1 nm photon. This means, a 656.1 nm photon has the spin speed of $\omega_{phot,ph}$ = 2.87E+15 arc/s. Notice that this spin speed value is exactly a 656.1 nm photon's frequency $f_{n,ph} = \omega_{n,ph}/(2\pi)$ = 4.57E+14 Hz (see Table 1 column 14, now we name it as a **photon's spin-frequency**). Similarly, from Table 1 column 23, we see that a 121.5 nm photon (that emitted from n=2 to n=1 electron transition) has the spin speed $\omega_{n=1,ph} - \omega_{n=2,ph}$ = 1.55E+16 arc/s, a 102.5 nm photon (that emitted from n=3 to n=1 electron transition) has the spin speed $\omega_{n=1,ph} - \omega_{n=3,ph}$ = 1.84E+16 arc/s, and both photons have the spin-frequencies equal to photon's frequency (see column 14).

If this hypothesis is correct, then above calculations brought us some new results:

1) Although all electrons are said to have either spin +½ $\hbar$ or spin –½ $\hbar$, in an H-atom, under the face-to-face tidal-locked binary model, a bound state electron in different n orbit should have different spin-speed (regardless of ±½$\hbar$). This means, an electron (in an H-atom) has its true value of spin-speed $\omega_{spin,elec} = \omega_{orbit\text{-}elec,ph}$ that completely depends on its n orbit QM state, and this n orbital rotation electron's spin-speed is the same as this electron's orbital rotation frequency. This is only for the atom-bound electrons. For the (unbound) free motion electrons, because its $r_n \to \infty$ relative to its "mother" atom's center, so its QM state equals to $n \approx \infty$, and its "orbital velocity" around its "mother" atom is $v_n = v_1/n = v_1/\infty \approx 0$. Thus, for the purpose of electron spin, a free electron's free motion speed cannot be treated as the orbital velocity.

2) Although all photons are always said to have spin +1$\hbar$, each photon should have its real value of spin-speed $\omega_{n,ph}$ that only depends on its wavelength or frequency. A photon's spin-speed equals to this photon's frequency (because of $\omega_{n,ph} = 2\pi f_{n,ph}$), and also equals to the ABCBA cycle frequency (see SunQM-6s5) of this photon. This means, different colored photon has different spin-speed, just like different colored photon has different frequency. For example, a 656.1 nm photon has frequency of $f_{phot,ph}$ = 4.57E+14 Hz, thus it has spin-frequency at 4.57E+14 Hz, or spin-speed $\omega_{phot,ph} = 2\pi f_{phot,ph}$ = 2.87E+15 arc/s (see Table 1); a 589 nm photon (that from a Sodium-vapor lamp) should have the spin-frequency at $f_{phot,ph} = c / \lambda_{phot,ph}$ = 5.09E+14 Hz, or spin-speed $\omega_{phot,ph} = 2\pi f_{phot,ph}$ = 3.20E+15 arc/s. Notice that a photon's spin frequency (or spin speed) can be intuitively depicted as the rotation frequency of an electric field $\vec{\mathbf{E}}$ vector between a nuclear proton and a virtual electron (that is doing orbital rotation at a virtual orbital number n") in an H-atom (see SunQM-6s1's Fig-1a). Notice that the spin vector of a photon is (initially, or originally) in perpendicular to the moving direction (see SunQM-6s5's Fig-5), although it can be reoriented to any new direction relative to the moving direction (see SunQM-6s5's section-V).

3) Similarly, (regardless to spin ±½$\hbar$), the real spin-speed of a nuclear proton in an H-atom completely depends on (or equals to) the spin-speed of the orbital moving electron (that face-to-face tidal locked in the binary orbital movement. Or similarly, based on the "proton-electron mirror-coupled orbit" model). This means, the n=3 to n=2 transition causes the increasing of spin-speed not only for the electron, but also for the proton. Because the nuclear proton is at almost the center of the reduced mass, the angular momentum change of the proton is only about 1/2000 of that of the electron. Then, for the moment, we can ignore it here. (Note: It is deduced as: For a proton-electron binary system, the reduced mass μ at $r_\mu = 0$, then $r_e m_e = r_p m_p \to r_p/r_e = m_e/m_p$; $v_e = \omega_e r_e$, $v_p = \omega_p r_p$, face-to-face tidal locked, $\omega_e = \omega_p$; Electron's angular momentum $|\vec{\mathbf{L}}_{\mathbf{elec}}|$ =

$m_e v_e r_e$, and proton's $|\vec{\mathbf{L}}_{\mathbf{prot}}| = m_p v_p r_p$, then, $\frac{L_p}{L_e} = \frac{m_p v_p r_p}{m_e v_e r_e} = \frac{m_p \omega_p r_p r_p}{m_e \omega_e r_e r_e} = \frac{m_p}{m_e}\left(\frac{r_p}{r_e}\right)^2 = \frac{m_p}{m_e}\left(\frac{m_e}{m_p}\right)^2 = \frac{m_e}{m_p} \approx \frac{1}{2000}$). (Note: In Figure 5a, due to the face-to-face tidal-locking, the proton has the same physical spin as electron, but due to the opposite charge, it has the opposite (electric) spin ↑↓, (because the spin of an electron or a proton is defined as the electric spin that may or may not be the same as the physical spin of the particle)).

4) According to the Bohr-QM formula [35],

$|\vec{\mathbf{L}}_{\mathbf{n,orbit}}| = mv_n r_n = n\hbar$, (where $\hbar = mv_1 r_1$, m is the mass) eq-27 (Bohr-QM formula)

the electron's orbital angular momentum $|\vec{\mathbf{L}}_{\mathbf{n,elec}}|$ in H-atom at each n orbit was calculated (see Table 1 column 24). Column 25 (of Table 1) showed the orbital angular momentum difference between n+1 and n (i.e., $\Delta|\vec{\mathbf{L}}_{\mathbf{(n+1)-n}}|$) for all different n (in a single N super shell), and they all have the same value as that of the $|\vec{\mathbf{L}}_{\mathbf{n=1}}|$ = 1.055E-34 (kg*m*m/s) = $\frac{h}{2\pi} = \hbar$. This is exactly what the Bohr-QM formula eq-27 means. Now I try to use this result to prove the hypothesis that "the face-to-face tidal locked binary orbital motion should be the default state for the orbital electron in an H-atom". Let's imagine that in n shell, one electron is evenly distributed in a small solid-cubic-bar-like 3D space within $r_n \le \Delta r \le r_{n+1}$, $\frac{\pi}{2} - \delta \le \Delta\theta < \frac{\pi}{2} + \delta$, and $-\delta \le \Delta\varphi < +\delta$. When this solid-cubic-bar (i.e., the "slave" object of the binary) doing the (binary) circular orbital motion in n orbital shell, its one end (at r_n) is always pointing to the circular orbit's center, and its another end (at r_{n+1}) is always pointing away from the circular orbit's center (due to $\Delta|\vec{\mathbf{L}}_{\mathbf{(n+1)-n}}| = +1\hbar$). Then, the n=1 spherical surface (i.e., the "master" object of the binary) is also self-spinning at $|\vec{\mathbf{L}}_{\mathbf{n=1}}| = +1\hbar$. Thus, after one round of circular motion, the "master" object (i.e,, the n=1 spherical surface) finishes one spin of $|\vec{\mathbf{L}}_{\mathbf{n=1}}| = +1\hbar$, and the "slave" object (i.e., the solid-cubic-bar) also finishes one spin of $|\vec{\mathbf{S}}_{\mathbf{n}}| = \Delta|\vec{\mathbf{L}}_{\mathbf{(n+1)-n}}| = +1\hbar$. Therefore, this analysis support that the "master" object and the "slave" object are naturally doing the face-to-face tidal locked binary orbital motion. Furthermore, not only Bohr-QM formula eq-27, but also Schrodinger equation/solution may can be used similarly to prove this hypothesis. (Note: If fixed at one end of the solid-cubic-bar, then this solid-cubic-bar has spin angular momentum of $+1\hbar$. However, if fixed at the (reduced mass) center of the solid-cubic-bar, then this solid-cubic-bar should have the spin angular momentum of $½\hbar$).

5) Noticed that an electron at n=1 orbit's inner edge r_1 = 5.29E-11 (meters) will have orbital angular momentum of $1\hbar$ = 1.05E-34 (kg*m*m/s), but the same electron at n=1 orbit's outer edge $r_2 = 4\times$ 5.29E-11 meters will have orbital angular momentum of $2\hbar$ = 2.11E-34 (kg*m*m/s). Because the electron has 100% occupancy in the orbital space between r_1 and r_2, neither of these two values can be used to accurately present an electron's orbital angular momentum in the n=1 orbital space, and the true value must be in between these two values. After averaging (by integrating) an electron's elliptical orbital angular momentum within n shell (with the perihelion at r_n and the aphelion at r_{n+1}), it showed that $|\vec{\mathbf{L}}_{\mathbf{n}}| \approx \left(n + \frac{1}{2}\right)\hbar$, and **as** $\mathbf{n \to \infty}$, $|\vec{\mathbf{L}}_{\mathbf{n}}| = \left(\boldsymbol{n} + \frac{\mathbf{1}}{\mathbf{2}}\right)\hbar$, (see Appendix C for the calculations). Following this analysis, the best values for a bound state electron's orbital angular momentum in the n = 1, 2, 3, … orbital shell spaces should be $\le \frac{3}{2}\hbar, \frac{5}{2}\hbar, \frac{7}{2}\hbar$, etc., (instead of the inner edge's values of $1\hbar$, $2\hbar$, $3\hbar$, etc.).

6) So, ultimately, what is the real meaning of the spin $½\hbar$ for an electron? First, the spin of $\pm½\hbar$ was determined in the Stern-Gerlach experiment for the free motion electrons, and these electrons must be in the $n \approx \infty$ QM state (relative to their "mother" atom's center), thus they have the orbital angular momentum $|\vec{\mathbf{L}}_{\mathbf{n}}| = \left(n + \frac{1}{2}\right)\hbar$. Second, during the free motion, these n state electrons are moving from the inner edge to the outer edge of the n shell (or from r_n to r_{n+1}), so, as we said previously, the difference of the orbital angular momentum between the two edges $\Delta|\vec{\mathbf{L}}_{\mathbf{(n+1)-n}}| = \frac{1}{2}\hbar$ is carried over by the electrons as their spin angular momentum $|\vec{\mathbf{S}}| = \frac{1}{2}\hbar$. This is the best explanation that I can give.

7) For photon's spin $+1\hbar$, it is clear that it comes from the electron's orbital angular momentum change from n+1 to n (in Bohr-QM, see Table 1), or more accurately, from the selection rule $\Delta l = \pm 1$ (in the Schrodinger equation/solution).

VII-c. For a pair of spin ↑↓ electrons, their (electron-proton) face-to-face tidal-locked orbital rotation in φ-1D (in the opposite ±m directions) may have transformed into a θ-1D uni-directional orbital rotation.

For one pair of spin ↑↓ electrons' orbital rotation trajectory, let's use Helium atom's two n=1 electrons (in $1s^2$ QM state) as the example. Due to their negative charged repulsive force, two electrons have the anti-parallel (electric) spin ↑↓. (Note: It is equivalent to the (proton-electron) positive-negative charge pair's parallel physical spin in H-atom). According to the Schrodinger equation's solution (i.e., the NBP, or the Y(*l*,*m*) function, for example, by comparing Y(l=1,m=1) = $-\sqrt{\frac{3}{8\pi}}e^{im\varphi}\sin\theta$, with, Y($l$=1,$m$=-1) = $\sqrt{\frac{3}{8\pi}}e^{-im\varphi}\sin\theta$), I guessed that these two ↑↓ spin n=1 electrons should be doing orbital rotation in opposite directions (meaning, one in +m direction, one in -m direction, both in φ-1D). As shown in Figure 5b, the blue line represent the orbital rotation trajectory of the electron-2 (that supposed to have the down-spin, and represented by the blue thick arrow ↓) that moving in +m direction (from -x axis to -y axis, or from position-6 to -7), and the red line represent the orbital rotation trajectory of the electron-1 (that has the up-spin, represented by the red thick arrow ↑) that moving in -m direction (from +x axis to -y axis, or from position-1 to -2). If they are continues moving like this (along the equator of the n=1 orbital shell), they will collide at the -y axis. However, the repulsive force of these two electrons will not only prevent this collide, but also will keep the farthest distance in between these two electron. Then one of these two electrons has to go through the north pole (let's assuming it is the red electron-1, from the position-1, to 2, 3, 4, 5), and the second one has to go through the south pole (let's assuming it is the blue electron-2, from position-6 to 7, 8, 9, 10). This is the explanation for Figure 5b.

Then let's explain the Figure 5c. Because the E/RFe repulsive force (between the two electrons in n=1 orbit shell space) is so strong, the distance (between the two electrons) smaller than the half circumference is not allowed at any time during the orbital rotation, so that the movement (of the electron-1 from position-1 to position-2 in -m direction in φ-1D, and the movement of the electron-2 from position-6 to position-7 in -m direction in φ-1D) in Figure 5b is not allowed (because the resulted distance between position-2 to position-7 is smaller than the half circumference). So, even at the beginning, the two electrons' ±m φ-1D orbital movement (along the equator, or along the latitude line) has to be along longitude line (in θ-1D), as shown in Figure 5c. Thus, an original φ-1D orbital rotation is now transformed into a θ-1D orbital rotation. After carefully tracing (in Figure 5c), we will find that both electrons' spin vectors (one is up at the initial position-1, and one is down at the initial position-6) will have to keep overlapping with the longitude line on the n=1 sphere and pointing in the same (circular tangential) direction at all time during the orbital movement. This is perfect to keep spin ↑↓ anti-parallel for these two electrons at all time. And it is also perfect to keep a half circumference distance between these two electrons at all time during the orbital movement.

I believed that we can also use eq-1 at n=1 ($v_{1,ph} = \frac{1}{2}v_{1,gr}$) to explain Figure 5c. At the initial state (let's define it as **state-1**), the electron-1 is at position-1 with spin-up, and the electron-2 is at position-6 with spin-down. After moving ½ circumference, the electron-1 moved to position-6 with spin-down and the electron-2 moved to position-1 with spin-up (let's define it as **state-2**). After moving the second ½ circumference, the electron-1 moves back to position-1 with spin-up and the electron-2 moved back to position-6 with spin-down, and thus, it goes back to state-1 and finishes one cycle. However, if the identity of these two electrons are indistinguishable (meaning electron-1 = electron-2), then state-2 equals to state-1 (because both have one electron at position-1 with spin-up and one electron at position-6 with spin-down), and thus, only ½ circumference will finish one cycle. Now let's define each individual electron's orbital velocity (in Figure 5b) as $v_{1,ph}$, and define the sum of the two electrons' orbital (relative) velocity (in Figure 5c) as $v_{1,gr}$, then we have $v_{1,gr} = 2v_{1,ph}$, that is, $v_{1,ph} = \frac{1}{2}v_{1,gr}$. (Note: Why I define $v_{1,ph}$ as each individual electron's orbital velocity? Because each individual electron's orbital velocity has either +m direction, or -m direction (see in Figure 5b), and this two opposite directional orbital wave

motion is more like a phase wave's behavior. Why I define $v_{1,gr}$ as the sum of the two electrons' orbital velocity? Because in Figure 5b, the opposite directional motion makes the relative speed between two electrons = $2v_{1,ph}$. Furthermore, as a group, these two electrons are indistinguishable (or, electron-1 = electron-2), thus, only ½ circumference will finish one cycle). If this explanation is correct, then the group velocity must correlate to a velocity of a group of electrons (with each electron's identity indistinguishable), and the phase velocity must correlate to a velocity of each single electron (with each electron's identity is distinguishable among any of other electrons).

One of the key results of this analysis is, a pure φ-1D orbital rotation (in ±m opposite directions) for a pair of spin ↑↓ electrons (with the spin vectors perpendicular to the orbital moving direction), under the repulsion, it will be transformed into a pure θ-1D orbital rotation (in uni-direction, with the both spin vectors lying in the orbital moving direction). This kind of dynamic space transformation, (i.e., φ-1D orbital rotation transformed into θ-1D orbital rotation), is similar as that we have seen before: a nLL's mode (in φ-1D space) transformed into nL0 (in pseudo r-1D space, see SunQM-6). This transformation of a pure φ-1D orbital rotation to a pure θ-1D orbital rotation may also be the origin of the RF.

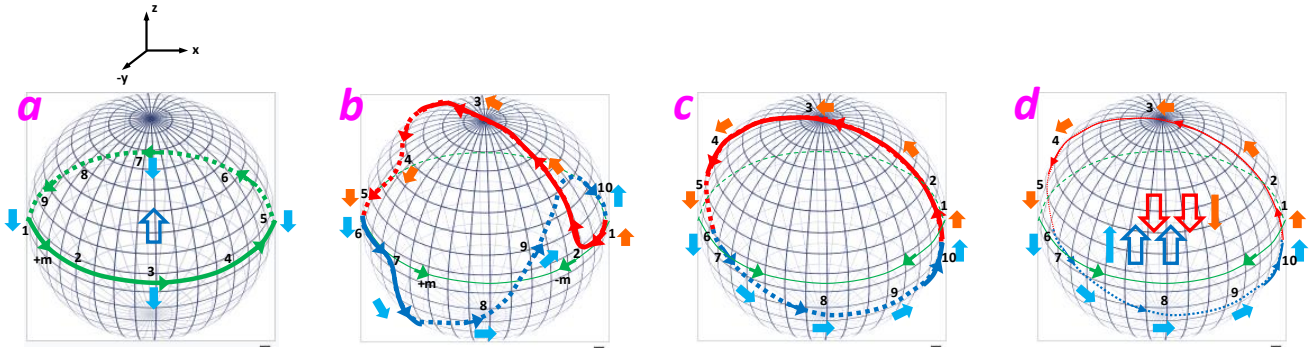

Figure 5a. One single electron is doing orbital rotation in an H-atom (with its spin face-to-face tidal-locked to proton's spin). The thick solid light-blue arrow represents electron's spin vector, the hollow dark-blue arrow represents proton's spin vector. Notice that the spin vector of electron is perpendicular to the orbital trajectory at all time.
Figure 5b. A pair of spin ↑↓ electrons in a He-atom (that are doing the opposite ±m orbital rotation in φ-1D) will be forced to go through two opposite poles to avoid the crash. The thick solid dark-orange arrow represents electron-1's spin vector, and the thick solid light-blue arrow represents electron-2's spin vector (both only for the first half cycle of the orbital rotation).
Figure 5c. A pair of spin ↑↓ electrons (that are doing the opposite ±m orbital rotation in φ-1D) will be eventually forced to do a pure θ-1D orbital rotation to avoid the crash. Notice that the spin vectors of electrons are now in-line within the orbital trajectory.
Figure 5d. A guessed spin configuration of (⇑⇑↑)(⇓⇓↓) for each of four nucleons in an alpha particle.

VII-d. A guessed spin configuration for each of four nucleons in an alpha particle

Inside an alpha particle, the E/RFe-force wants to separate the two protons as far as possible. So, I guessed that this caused the even-stronger S/RFs-force to bind one neutron to one proton (but not the two neutrons nor the two protons) to form a sub-structure. Thus, I guessed that there are two neutron-proton pairs of sub-structures inside one alpha particle, and here we name them as **neutron-proton-pair-1**, and, **neutron-proton-pair-2**. Within each one neutron-proton pair, the face-to-face tidal-locked orbital rotation around the reduced mass center (of this neutron-proton pair) makes these two nucleons to have spin in parallel, for example, ⇑⇑, (let's use ⇑ to represent **each nucleon's internal spin**, and use ↑ to represent **each nuclear proton's electric spin and each electron's spin**). Then, after adding the E/RFe-force field spin of the proton (that ↑ should be in the same direction as this proton's nucleon spin direction ⇑ because of proton has the positive charge), one pair of neutron-proton will have spin of either ⇓⇓↓ or ⇑⇑↑. Then, I guessed that two pairs of neutron-proton will have the spin configuration of (⇑⇑↑)(⇓⇓↓), or, in anti-parallel (see Figure 5d). (Note: Although the RFs-RFs interaction is stronger than

the RFe-RFe interaction, the RFs-RFs interaction is already consumed by the two nucleons (within one neutron-proton pair)'s ⇑⇑ spin-spin interaction, so the leftover RFs-force (we named it as the **residue RFs-force**) of the neutron-proton-pair-1 that can be used to interact with the residue RFs-force of the neutron-proton-pair-2 become weak, and it is guessed even weaker than the RFe-RFe interaction force between the two pairs of neutron-proton (because that the RFe-force of each pair of neutron-proton has not been consumed). In this case, the RFe-RFe interaction force overcome the residue RFs-force, and caused (⇑⇑↑)(⇓⇓↓) spin configuration for the four nucleons inside an alpha particle). (Note: If the residue RFs-force still overcome the RFe-RFe interaction, then it would become (⇑⇑↑)(⇑⇑↑), then two parallel spin ↑↑ protons inside the nucleus would be unable to match the two anti-parallel spin ↑↓ electrons to do the face-to-face tidal-locked orbital rotation).

If the face-to-face tidal-locked theory is correct, then the neutron-proton-pair-1 (suppose it has spin ⇓⇓↓) will have to face-to-face tidal-locked with electron-1 (with spin ↑) to do the binary orbital rotation, and simultaneously, the neutron-proton-pair-2 (that must have spin ⇑⇑↑) will have to face-to-face tidal-locked with electron-2 (with spin ↓) to do the binary orbital rotation. (Note: proton ↓ electron ↑ means these two particles are physically spinning in parallel ↑↑, so it becomes face-to-face tidal-locked). Then, because electron-1's and electron-2's φ-1D orbital rotation (in ±m opposite directions) has been transformed into a pure θ-1D orbital rotation (in uni-direction), the neutron-proton-pair-1's and the neutron-proton-pair-2's φ-1D orbital rotation inside the nucleus (in ±m opposite directions, with the spin vectors of ⇓⇓↓ and ⇑⇑↑ perpendicular to the orbital motion direction) must also have been transformed into a pure θ-1D orbital rotation (in uni-direction, with the spin vectors of ⇓⇓↓ and ⇑⇑↑ lying in the orbital moving direction). This explanation also fits to the "proton-electron mirror-coupled orbit" model.

(Note: In a Helium atom, among three levels of face-to-face tidal-locked binary motions, that is, the strongest S/RFs within each neutron-proton-pair, the second strongest E/RFe between neutron-proton-pair-1 to neutron-proton-pair-2, and the third strongest E/RFe between each proton-electron-pair, I guessed that it should be the neutron-proton pair's orbital rotation at inside the nucleus that drives the electron's orbital movement at outside the nucleus, and not the opposite way). (Note: Because the major spin is around each neutron-proton-pair, and the minor spin is around two of neutron-proton-pairs that formed a pseudo alpha particle, so for the spins in a large Z# (atomic number) nucleus (that supposed to have many pseudo alpha articles inside it), there is not much difference between the pseudo alpha particle that at the center, or at the surface of the nucleus). (Note: In this case, the Pauli principle of electric spin ↑↓ is actually driven by the global E/RFe electric energy minimization).

(Note: The Schrodinger equation for a proton-electron system (in an H-atom) may can be constructed, and it may also include the spin information. See Appendix D for details).

VIII. The possible origin of the Sun's spin and the planet's spin

First, for the Solar system, there is no more one-to-one face-to-face tidal-locking, simply because there are many "slave" planets and only one "master" Sun. Instead, the Solar system's spin-reference-frame may follow SunQM-3s1's eq-1, $\omega_{n\text{-spin}} = \omega_{1\text{-spin}} / n\text{^}x$, where x is a real number within $1 \le x \le 4$.

The origin of the spin of our Sun had been guessed in SunQM-3s2, "*An orphan Jupiter-sized planet (or even a red dwarf) flew by pass the nebula and was captured by one of these local mass centers; Spiraled in and then super positioned to the local mass center, this orphan planet seeded a formation of our pre-Sun ball, and determined our Solar system's spin axis direction and angular momentum*".

There are two different ways to explain the initial spin of all planets in our Solar system: one using classical physics (see Figure 6), and one using Bohr-QM (see Table 4 columns 13~17).

Here is the first way for the explanation. According to the {N,n} QM theory, for our pre-Sun ball, after a major collapsing of the N super-shell matter, > 99% of mass in this N super shell (including {N,n=1..5//6}o orbital shells) was collapsed into the N-1 super shell, and only < 1% mass was leftover in each of the n orbital spherical shells (see SunQM-1s1). In view of the classical physics, the spinning of the pre-Sun ball made the matter at the equator to move outward a little bit to form an oblate shape (for the pre-Sun ball at both N super shell and N-1 super shell, see the "step-1" in Figure 6a).

Meanwhile the nLL-force (see SunQM-3s1's "nLL effect") pushed the matter from the high latitude to the equator at the inner edge of the n orbital shell, and the higher the latitude it come from, the inner the edge it will go (see the "step-2" in Figure 6a). All mass in the same n orbital shell should have same spin frequency $\omega_{n,spin}$ along z-axis (see SunQM-3s1's eq-1), and the higher the latitude, the short the distance from the spin axis the mass location (see d', d", and d"' in Figure 6a), the slower the tangential velocity it will be ($v_{n,spin} = \omega_{n,spin} \times d$). So, after fully disk-lyzed (to $\theta = \pi/2$), in the same n orbital shell disk, the mass in the inner edge will have the slower tangential velocity than that of the mass in the outer edge. (Note: Because all mass in n shell should have the same $v_{n,gr,orbit}$ to start with, the newly added $v_{n,spin}$ is a smaller value than the initial $v_{n,gr,orbit}$. Also see the similar explanation in SunQM-3s9's Fig-5b). After accreting all mass in this n orbital shell, this difference of the tangential velocity causes the formed planet to have the spin direction in the same spin direction of the Sun, and also in the same direction of its own orbital rotation (see Figure 6b). In this way, all eight original planets (or twelve planets, if including the {3,2} {3,3}, {3,4}, {3,5} undiscovered ones) should have their original spin vectors in the same spin direction of the Sun. (Note: I figured out this explanation in 2018).

Here is the second way for the explanation. (Note: If a pre-Sun ball collapsed and only formed a single planet, then the explanation in Table 4 may provide a perfect mechanism for the formation of the face-to-face tidal-locked binary system. Here is a citizen-scientist-leveled prove). According to the {N,n} QM theory, suppose a {N,n=1..5//6}o = {N+1,1//6} sized spinning pre-Sun ball collapsed to a {N,1//6} = {N-1,n=1..5//6}o sized spinning pre-Sun ball, at the surface equator of this new {N,n=1//6} sized spinning pre-Sun ball, it should have the spin frequency of $\omega_{spin,n=1}$. Then, according to the Bohr-QM formula of eq-27, but wait, according to SunQM-2, in the macro-world {N,n} QM, we need to use the h_{gen} to replace the Planck constant h (for both Bohr-QM and Schrodinger-QM). Thus, for the pre-Sun ball (or the Solar system), eq-27 becomes

$$\left|\vec{\mathbf{L}}_{\mathbf{n,orbit}}\right| = mv_n r_n = n[(Hm)/(2\pi)] = n\hbar_{gen} \qquad \text{eq-28 (Bohr-QM formula for pre-Sun ball)}$$

where H=h/m' is the "quasi-Planck constant", m' is a scaling factor (with unit of mass), m is the mass of the object, h_{gen} = Hm is the "general Planck constant", and $\hbar_{gen} = \frac{Hm}{2\pi} = mv_1 r_1$ (see SunQM-2's section I-c). Then, according to the Bohr-QM formula of eq-28, at the surface equator of this n=1 sized pre-Sun ball (i.e., the "master" of the binary), it has the orbital angular momentum at n=1, or $\left|\vec{\mathbf{L}}_{\mathbf{n=1,pre-Sun,orbit}}\right| = mv_n r_n = n\hbar_{gen} = +1\hbar_{gen}$, that also equals to this pre-Sun ball's spin angular momentum $\left|\vec{\mathbf{S}}_{\mathbf{pre-Sun,spin}}\right| = \left|\vec{\mathbf{L}}_{\mathbf{n=1,pre-Sun,orbit}}\right| = +1\hbar_{gen}$. Then, let's assuming that among n= 2, 3, 4, 5 shells, only one n shell has < 1% mass left, the rest three of n shells have zero mass left. (Note: During the pre-Sun ball collapsing and disk-lysing, the n=1 orbital shell between $r_{n=1}$ to $r_{n=2}$ must be empty because of the "ball-torus-6-11-gap effect", see SunQM-1s1's section-V). Under the same Bohr-QM, the mass at the inner edge of this n orbital shell has the orbital angular momentum $\left|\vec{\mathbf{L}}_{\mathbf{n,orbit}}\right| = n\hbar_{gen}$, and the mass at the outer edge of this n orbital shell has the orbital angular momentum $\left|\vec{\mathbf{L}}_{\mathbf{n+1,orbit}}\right| = (n+1)\hbar_{gen}$. So, there is a difference of the orbital angular momentum $\Delta\left|\vec{\mathbf{L}}_{\mathbf{(n+1)-n,orbit}}\right| = (n+1)\hbar_{gen} - n\hbar_{gen} = +1\hbar_{gen}$ between the mass (in the same n shell) at the n edge and n+1 edge. After accreting all mass in this n orbital shell, the newly formed planet (i.e., the "slave" of the binary) must be located at the inner edge of the n orbital shell (because it has < 1% mass occupancy in the n orbital shell), so that it must have the orbital angular momentum $\left|\vec{\mathbf{L}}_{\mathbf{n,orbit}}\right| = mv_n r_n = n\hbar_{gen}$. Then, the differential orbital angular momentum $\Delta\left|\vec{\mathbf{L}}_{\mathbf{(n+1)-n,orbit}}\right| = +1\hbar_{gen}$ is carried over by the newly formed planet as the spin angular momentum $\left|\vec{\mathbf{S}}_{\mathbf{planet,spin}}\right| = \Delta\left|\vec{\mathbf{L}}_{\mathbf{(n+1)-n,orbit}}\right| = +1\hbar_{gen}$, with the spin vector in the same direction as that of the orbital angular momentum's vector $\left|\vec{\mathbf{L}}_{\mathbf{n,orbit}}\right| = n\hbar_{gen}$. Now, after the circular orbital rotation for one complete around, both the "master" pre-Sun (at the size of n=1) and the "slave" planet (at the orbit of n) have a complete spin of $+1\hbar_{gen}$, therefore they must be in a face-to-face tidal-locked binary motion. (Note: In this case, we ignored "the closed arm makes the skater's body spin faster" effect for the accretion of the planet).

(Note: Why here we use Bohr-QM? Because for the < 1% leftover mass, the RF is completely removed, so it should can be described by the Bohr-QM).

Now let's explain the data in Table 4. Columns 1 ~12 were copied from Table 2. Column 13 showed that after the N super shell of the pre-Sun ball collapsed, and after the < 1% leftover mass disk-lyzed, the orbital angular momentum of 1 kg

mass (or per 1 kg) at each r_n , i.e., $|\vec{\mathbf{L}}_{\mathbf{n,orbit}}| = mr_nv_{r,gr}/m = r_nv_{r,gr}$. Column 14 showed the difference of $|\vec{\mathbf{L}}_{\mathbf{n,orbit}}|$ at r_{n+1} and r_n for this 1 kg mass, notice that it equals to H/(2π). To confirm it, multiplying column 14 by 2π becomes column 15, and notice that the yellow cells (9.55E+14 J*s/kg) in column 15 equals to Table 2's column 16, the green cells (5.73E+15 J*s/kg) in column 15 equals to Table 2's column 22. (Note: the blue cells in column 15 does not equal to Table 2's column 28 (3.44E+16 J*s/kg), because the "period factor" it used was 5.33, not 6, (see Table 4 column 8). If had used 6, then the blue cells in column 15 would have equaled to Table 2's column 28). Then, the physical meaning of Table 4's column 13 ~ 17 is exactly the Bohr-QM formula of eq-28. Columns 16 ~ 17 were used to check for eq-28: When the pre-Sun ball collapsed (from {2,1//6} size) to {1,1//6} size, and after disk-lyzed, 1 kg of mass at either $r_{n=1}$ = {1,1//6} nLL orbit, or $r_{n=2}$ = {1,2//6} nLL orbit, or $r_{n=3}$ = {1,3//6} nLL orbit, or up to $r_{n=6}$ = {1,6//6} nLL orbit, will have the orbital angular momentum of n=1, 2, 3, … 6 (see column 17), with the unit of H/(2π) = 9.12E+14 (J*s/kg), and this unit is same as the $|\vec{\mathbf{L}}_{\mathbf{n=1,orbit}}|$ at N=1; When the pre-Sun ball collapsed (from {1,1//6} size) to {0,1//6} size, and after disk-lyzed, 1 kg of mass at either $r_{n=1}$ = {0,1//6} nLL orbit, or $r_{n=2}$ = {0,2//6} nLL orbit, or $r_{n=3}$ = {0,3//6} nLL orbit, or up to $r_{n=6}$ = {0,6//6} nLL orbit, will have the orbital angular momentum of n=1, 2, 3, … 6 (see column 16, top cells), with the unit of H/(2π) = 1.52E+14 (J*s/kg), and this unit is same as the $|\vec{\mathbf{L}}_{\mathbf{n=1,orbit}}|$ at N=0. (Note: In this sense, H= 3.44E+16 J*s/kg may be not perfect for {2,n=1..5//6}o super shell, because it does not bring $L_{n,orbit} = n(Hm)/(2\pi)$ into integer number of n, see column 16 of Table 4, bottom cells).

Columns 18 of Table 4 showed the planet size of the original planets (that copied from SunQM-3s6's Table-2 column-11). Based on the rule of "all mass between r_n and r_{n+1} belongs to orbit n (see paper SunQM-3s2)", and assuming that during the accretion 1 kg of mass from the outer edge of n shell at r_{n+1} is brought to the planet's far site surface (relative to the Sun) and still carries its original orbital angular momentum $|\vec{\mathbf{L}}_{\mathbf{n+1,orbit}}|$, and 1 kg of mass from the inner edge of n shell at r_n is brought to the planet's near site surface and still carries its original orbital angular momentum $|\vec{\mathbf{L}}_{\mathbf{n,orbit}}|$, then, column 19 of Table 4 calculated if these two (1 kg) objects paired (with the distance of the planet's diameter in column 18) and then doing binary circular orbital rotation, and then, what is the tangential speed of this binary circular orbital rotation. Finally, column 20 of Table 4 calculated the period of this two (1 kg) objects' binary circular orbital rotation. The result was 1 ~ 15 seconds, too fast in comparison with the known spin-period of the eight planets. The reason of the un-match is obvious: a planet at r_n accretes most of the mass from nearby r_n, the mass accreted from r_{n+1} is negligible. With this in mind, I made the re-calculation by assuming that the 2nd 1 kg mass is not accreted from r_{n+1}, but from $r_n + \Delta r$. Using Neptune as the example (because among all eight planets, Neptune is the only one that still keeps the original mass, see SunQM-1s1), it showed that if the 2nd 1 kg mass is originally at $r_n + \Delta r$ = 4.45E+12 (meters) + 3.66E+7 (meters), and it is accreted to Neptune's far site surface $r_n + r_{Neptune}$ = 4.45E+12 (meters) + 2.00E+7 (meters), then the resulted two of 1 kg objects binary will have the circular orbit rotation period ≈ 5.0E+4 (sec) ≈ 16.1 days, the same spin period of Neptune. This result supported the previous saying: a planet at r_n accretes most of the mass from nearby r_n . (Note: A more sophisticated method was explored, but not finished, and thus was not shown here).

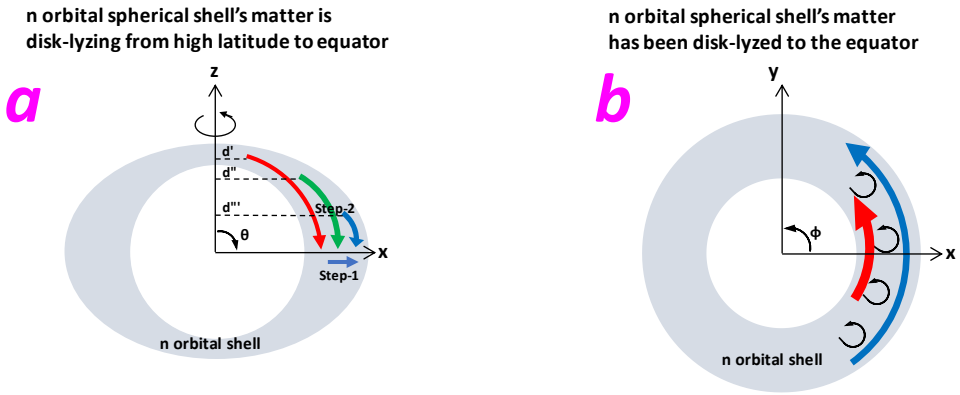

Figure 6a. Illustration of how an n orbital spherical shell's matter (in a newly collapsed pre-Sun ball) is disk-lyzing (to form a disk-shape) from the high latitude to the equator (viewed in xz-2D).

Figure 6b. Illustration of how the differential orbital angular momentum at the inner and outer edge of the same n shell will cause all objects (in the n shell) to do the spin (in the same direction of orbital rotation, viewed in xy-2D).

Table 4. To show that the initial spin of all original planets in our Solar system follows Bohr-QM.

NASA's data of planets					{N,n} QM model calculated data							orbit angular momentum					planet spin angular momentum		
	mass	Sun's radius or planet orbit-r	planet orbit-v	**classic orbit E=-(1/2)mv²**	N=	n=	period factor=	total n=	$r_n=r_1n^2$	$v_{n,gr}$ = sqrt(GM/r_n)	{N,n} QM E_n=**-(1/2) $mv_{n,gr}^2$**	L_n= $mr_nv_{n,gr}$/m (per kg)	ΔL_n= L_{n+1}-L_n = H/(2π) (per kg)	H=h/m' (per kg)	$L_n/\Delta L_n$= L_n/(H/(2π))	$L_n/\Delta L_n$= L_n/(H/(2π))	original r_{planet} (from model)	planet equator tangential speed v_{spin} = $(\Delta L_n/2)/r_{planet}$	planet's max spin period = $2\pi r_{planet}/v_{spin}$
unit	kg	meter	m/s	J					meter	m/s	J	meter*m/s *(kg/kg)	meter*m/s *(kg/kg)	J.s/kg			meter	m/s	s
Sun core		1.74E+08			0	1	6	1	1.74E+08	873647		1.52E+14	1.52E+14	9.55E+14	1				
SUN	1.99E+30	6.96E+08			0	2	6	2	6.96E+08	436824		3.04E+14	1.52E+14	9.55E+14	2				
					0	3	6	3	1.57E+09	291216		4.56E+14	1.52E+14	9.55E+14	3				
					0	4	6	4	2.78E+09	218412		6.08E+14	1.52E+14	9.55E+14	4				
					0	5	6	5	4.35E+09	174729		7.60E+14	1.52E+14	9.55E+14	5				
					1	1	6	6	6.26E+09	145608		9.12E+14	9.12E+14	5.73E+15	6	1			
					1	2	6	12	2.50E+10	72804		1.82E+15	9.12E+14	5.73E+15		2	3.36E+07	1.36E+07	15.59
Mercury	3.30E+23	5.79E+10	47400	**-3.71E+32**	1	3	6	18	5.64E+10	48536	**-3.89E+32**	2.74E+15	9.12E+14	5.73E+15		3	2.98E+07	1.53E+07	12.28
Venus	4.87E+24	1.08E+11	35000	**-2.98E+33**	1	4	6	24	1.00E+11	36402	**-3.23E+33**	3.65E+15	9.12E+14	5.73E+15		4	2.76E+07	1.65E+07	10.46
Earth	5.97E+24	1.49E+11	29800	**-2.65E+33**	1	5	6	30	1.57E+11	29122	**-2.53E+33**	4.56E+15	9.12E+14	5.73E+15		5	2.58E+07	1.76E+07	9.20
Mars	6.42E+23	2.28E+11	24100	**-1.86E+32**	2	1	6	36	2.25E+11	24268	**-1.89E+32**	5.47E+15	4.25E+15	2.67E+16	1.00	6			
Jupiter	1.90E+27	7.78E+11	13100	**-1.63E+35**	2	2	5.33	64.0	7.12E+11	13659	**-1.77E+35**	9.72E+15	4.86E+15	3.05E+16	1.78		3.04E+07	8.00E+07	2.38
Saturn	5.68E+26	1.43E+12	9700	**-2.67E+34**	2	3	5.33	95.9	1.60E+12	9106	**-2.35E+34**	1.46E+16	4.86E+15	3.05E+16	2.67		2.53E+07	9.61E+07	1.65
Uranus	8.68E+25	2.97E+12	6800	**-2.01E+33**	2	4	5.33	127.9	2.85E+12	6830	**-2.02E+33**	1.94E+16	4.86E+15	3.05E+16	3.55		2.22E+07	1.09E+08	1.28
Neptune	1.02E+26	4.51E+12	5400	**-1.49E+33**	2	5	5.33	159.9	4.45E+12	5464	**-1.52E+33**	2.43E+16	4.86E+15	3.05E+16	4.44		2.00E+07	1.22E+08	1.03
Pluto	1.46E+22	5.91E+12	4700	**-1.61E+29**	2	6	5.33	191.9	6.40E+12	4553	**-1.51E+29**	2.92E+16							
														this is different					

Conclusion

For matter wave, $v_{n,ph} = \frac{n}{2} v_{n,gr}$ is the more Eigen description than $v_{n,ph} = \frac{1}{2} v_{n,gr}$. The paired (up/down) spin information of the electron may have already been presented by the positive/negative wave peaks in either the Schrodinger equation/solution (in form of the non-Born probability), or in the de Broglie wave in the Bohr H-atom model. The spin of electron and nucleon may be originated from the face-to-face tidal-locked binary circular orbital rotation between them.

Acknowledgements (of all SunQM series articles):

Many thanks to: all the (related) experimental scientists who produced the (related) experimental data, all the (related) theoretical scientists who generated all kinds of theories (that become the foundation of {N,n//q} QM theory), the (related) text book authors who wrote down all results into a systematic knowledge, the (related) popular science writers who simplified the complicated modern physics results into a easily understandable text, the (related) Wikipedia writers who presented the knowledge in a easily accessible way, the (related) online (video/animated) course writers/programmers who presented the abstract knowledge in an intuitive and visually understandable way. Also thanks to NASA and ESA for opening some basic scientific data to the public, so that citizen scientists (like me) can use it. Also thanks to the online preprinting serve vixra.org to let me to post out my original SunQM series research articles.

Special thanks to: Fudan university, theoretical physics (class of 1978, and all teachers), it had made my quantum mechanics study (at the undergraduate level) become possible. Also thanks to Chen-Ning Yang and Tsung-Dao Lee, they made me to dream to be a theoretical physicist when I was eighteen. Also thanks to Shoucheng Zhang (张首晟, Physics Prof. at Stanford Univ., my classmate at Fudan Univ. in 1978) who had helped me to introduce the {N,n} QM theory to the scientific community in 2018.

Also thanks to a group of citizen scientists for the interesting, encouraging, inspiring, and useful (online) discussions: "职老" (https://bbs.creaders.net/rainbow/bbsviewer.php?trd_id=1079728), "MingChen99" (https://bbs.creaders.net/tea/bbsviewer.php?trd_id=1384562), "zhf" (https://bbs.creaders.net/tea/bbsviewer.php?trd_id=1319754), Yingtao Yang (https://bbs.creaders.net/education/bbsviewer.php?trd_id=1135143), "tda" (https://bbs.creaders.net/education/bbsviewer.php?trd_id=1157045), etc.

Also thanks to: Takahisa Okino (Correlation between Diffusion Equation and Schrödinger Equation. Journal of Modern Physics, 2013, 4, 612-615), Phil Scherrer (Prof. in Stanford University, who explained WSO data to me (in email, see SunQM-3s9)), Jing Chen

(https://www.researchgate.net/publication/332351262_A_generalization_of_quantum_theory), etc. Note: if I missed anyone in the current acknowledgements, I will try to add them in the SunQM-9s1's acknowledgements.

Reference:

[1] Yi Cao, SunQM-1: Quantum mechanics of the Solar system in a {N,n//6} QM structure. http://vixra.org/pdf/1805.0102v2.pdf （original submitted on 2018-05-03）
[2] Yi Cao, SunQM-1s1: The dynamics of the quantum collapse (and quantum expansion) of Solar QM {N,n} structure. http://vixra.org/pdf/1805.0117v1.pdf （submitted on 2018-05-04）
[3] Yi Cao, SunQM-1s2: Comparing to other star-planet systems, our Solar system has a nearly perfect {N,n//6} QM structure. http://vixra.org/pdf/1805.0118v1.pdf （submitted on 2018-05-04）
[4] Yi Cao, SunQM-1s3: Applying {N,n} QM structure analysis to planets using exterior and interior {N,n} QM. http://vixra.org/pdf/1805.0123v1.pdf （submitted on 2018-05-06）
[5] Yi Cao, SunQM-2: Expanding QM from micro-world to macro-world: general Planck constant, H-C unit, H-quasi-constant, and the meaning of QM. http://vixra.org/pdf/1805.0141v1.pdf （submitted on 2018-05-07）
[6] Yi Cao, SunQM-3: Solving Schrodinger equation for Solar quantum mechanics {N,n} structure. http://vixra.org/pdf/1805.0160v1.pdf （submitted on 2018-05-06）
[7] Yi Cao, SunQM-3s1: Using 1st order spin-perturbation to solve Schrodinger equation for nLL effect and pre-Sun ball's disk-lyzation. http://vixra.org/pdf/1805.0078v1.pdf （submitted on 2018-05-02）
[8] Yi Cao, SunQM-3s2: Using {N,n} QM model to calculate out the snapshot pictures of a gradually disk-lyzing pre-Sun ball. http://vixra.org/pdf/1804.0491v1.pdf （submitted on 2018-04-30）
[9] Yi Cao, SunQM-3s3: Using QM calculation to explain the atmosphere band pattern on Jupiter (and Earth, Saturn, Sun)'s surface. http://vixra.org/pdf/1805.0040v1.pdf （submitted on 2018-05-01）
[10] Yi Cao, SunQM-3s6: Predict mass density r-distribution for Earth and other rocky planets based on {N,n} QM probability distribution. http://vixra.org/pdf/1808.0639v1.pdf (submitted on 2018-08-29)
[11] Yi Cao, SunQM-3s7: Predict mass density r-distribution for gas/ice planets, and the superposition of {N,n//q} or |qnlm> QM states for planet/star. http://vixra.org/pdf/1812.0302v2.pdf (replaced on 2019-03-08)
[12] Yi Cao, SunQM-3s8: Using {N,n} QM to study Sun's internal structure, convective zone formation, planetary differentiation and temperature r-distribution. http://vixra.org/pdf/1808.0637v1.pdf (submitted on 2018-08-29)
[13] Yi Cao, SunQM-3s9: Using {N,n} QM to explain the sunspot drift, the continental drift, and Sun's and Earth's magnetic dynamo. http://vixra.org/pdf/1812.0318v2.pdf (replaced on 2019-01-10)
[14] Yi Cao, SunQM-3s4: Using {N,n} QM structure and multiplier n' to analyze Saturn's (and other planets') ring structure. http://vixra.org/pdf/1903.0211v1.pdf (submitted on 2019-03-11)
[15] Yi Cao, SunQM-3s10: Using {N,n} QM's Eigen n to constitute Asteroid/Kuiper belts, and Solar {N=1..4,n} region's mass density r-distribution and evolution. http://vixra.org/pdf/1909.0267v1.pdf (submitted on 2019-09-12)
[16] Yi Cao, SunQM-3s11: Using {N,n} QM's probability density 3D map to build a complete Solar system with time-dependent orbital movement. https://vixra.org/pdf/1912.0212v1.pdf (original submitted on 2019-12-11)
[17] Yi Cao, SunQM-4: Using full-QM deduction and {N,n} QM's non-Born probability density 3D map to build a complete Solar system with orbital movement. https://vixra.org/pdf/2003.0556v2.pdf (replaced on 2021-02-03)
[18] Yi Cao, SunQM-4s1: Is Born probability merely a special case of (the more generalized) non-Born probability (NBP)? https://vixra.org/pdf/2005.0093v1.pdf (submitted on 2020-05-07)
[19] Yi Cao, SunQM-4s2: Using {N,n} QM and non-Born probability to analyze Earth atmosphere's global pattern and the local weather. https://vixra.org/pdf/2007.0007v1.pdf (submitted on 2020-07-01)
[20] Yi Cao, SunQM-5: Using the Interior {N,n//6} QM to Describe an Atom's Nucleus-Electron System, and to Scan from Sub-quark to Universe (Drafted in April 2018). https://vixra.org/pdf/2107.0048v1.pdf （submitted on 2021-07-06)
[21] Yi Cao, SunQM-5s1: White Dwarf, Neutron Star, and Black Hole Explained by Using {N,n//6} QM (Drafted in Apr. 2018). https://vixra.org/pdf/2107.0084v1.pdf （submitted on 2021-07-13)
[22] Yi Cao, SunQM-5s2: Using {N,n//6} QM to Explore Elementary Particles and the Possible Sub-quark Particles. https://vixra.org/pdf/2107.0104v1.pdf (submitted on 2021-07-18)
[23] Yi Cao, SunQM-6: Magnetic force is the rotation-diffusion (RF) force of the electric force, Weak force is the RF-force of the Strong force, Dark Matter may be the RF-force of the gravity force, according to a newly designed {N,n} QM field theory. https://vixra.org/pdf/2010.0167v1.pdf (replaced on 2020-12-17, submitted on 2020-10-21)
[24] Yi Cao, SunQM-6s1: Using Bohr atom, {N,n} QM field theory, and non-Born probability to describe a photon's emission and propagation. https://vixra.org/pdf/2102.0060v1.pdf (submitted on 2021-02-11)
[25] Yi Cao, SunQM-7: Using {N,n} QM, Non-Born-Probability (NBP), and Simultaneous-Multi-Eigen-Description (SMED) to describe our universe. https://vixra.org/pdf/2111.0086v1.pdf (submitted on 2021-11-17)

[26] Yi Cao, SunQM-6s2: A Unified Description Of 1D-Wave, 1D-Wave Packet, 3D-Wave, 3D-Wave Packet, and |nlm> Elliptical Orbit For A Photon's Emission and Propagation Using {N,n} QM. https://vixra.org/pdf/2208.0039v1.pdf (submitted on 2022-08-08)
[27] Yi Cao, SunQM-6s3: Using {N,n} QM and "|nL0> Elliptical/Parabolic/Hyperbolic Orbital Transition Model" to Describe All General "Decay" Processes (Including the Emission of a Photon, a G-photon, or An Alpha-particle). (submitted on 2022-08-31, but has not been able to get posted out, I asked many times, no reply)
[28] Yi Cao, SunQM-6s4: In {N,n} QM Field Theory, A Point Charge's Electric Field Can Be Represented by Either the Schrodinger Equation/Solution, Or A 3D Spherical Wave Packet, In Form of Born Probability. https://vixra.org/pdf/2306.0136v1.pdf (submitted on 2023-06-23)
[29] Yi Cao, SunQM-6s5: Using {N,n} QM Field Theory to Describe A Propagating Photon as A 3D Spherical Wave Packet with the Oscillation Among Three QM States. https://vixra.org/pdf/2307.0098v1.pdf (submitted on 2023-07-18)
[30] Yi Cao, SunQM-6s6: Using {N,n} QM Field Theory to Study the Atomic Electron Configuration, the Pre-Sun Ball's {N,n} QM Structural Configuration, and the Nuclear Proton Configuration. https://vixra.org/pdf/2308.0118v1.pdf (submitted on 2023-08-18)
[31] David J. Griffiths, "Introduction to Quantum Mechanics", 2nd ed., 2015, pp66, eq-2.108.
[32] John S. Townsed, "A Modern Approach to Quantum Mechanics", 2nd ed., 2012, pp 180, eq-5.34.
[33] Douglas C. Giancoli, Physics for Scientists & Engineers with Modern Physics, 4th ed. 2009, p1010, Fig-37-29.
[34] In one explanation of the article "Observation of optical polarization Möbius strips", it said: "The Möbius strips show how the electric field is oriented at each position on a circular path surrounding the axis of the laser beam. Depending on the particulars of the structure of laser beam, the researchers observe Möbius strips of polarization having 3/2 or 5/2 twists. These strips demonstrate the rich structure that a light beam can possess at very small, subwavelength distance scales, Boyd explained". (https://phys.org/news/2015-01-mobius-experimentally-polarization.html). Also see: Bauer, Thomas; Banzer, Peter; Karimi, Ebrahim; Orlov, Sergej; Rubano, Andrea; Marrucci, Lorenzo; Santamato, Enrico; Boyd, Robert W.; Leuchs, Gerd (February 2015). "Observation of optical polarization Möbius strips". Science. 347 (6225): 964–966.
[35] Douglas C. Giancoli, Physics for Scientists & Engineers with Modern Physics, 4th ed. 2009, p1004, eq-37-10.

Note: A series of SunQM papers that I am working on:
SunQM-6s8: {N,n} QM Field Theory Development On the E/RFe-force and G/RFg-force … (drafted in Apr. 2023).
SunQM-6s9: {N,n} QM Field Theory Development On the S/RFs-force … (drafted in May. 2023).
SunQM-6s10: Schrodinger equation and {N,n} QM ... (drafted in January 2020).
SunQM-4s4: More explanations on non-Born probability (NBP)'s positive precession in {N,n}QM.
SunQM-7s1: Relativity and non-linear {N,n} QM
SunQM-9s1: Addendums, Updates and Q/A for SunQM series papers.

Note: Major QM books, data sources, software I used for SunQM series papers study:
Douglas C. Giancoli, Physics for Scientists & Engineers with Modern Physics, 4th ed. 2009.
David J. Griffiths, Introduction to Quantum Mechanics, 2nd ed., 2015.
Stephen T. Thornton & Andrew Rex, Modern Physics for Scientists and Engineers, 3rd ed. 2006.
John S. Townsend, A Modern Approach to Quantum Mechanics, 2nd ed., 2012.
Wikipedia at: https://en.wikipedia.org/wiki/
(Free) online math calculation software: WolframAlpha (https://www.wolframalpha.com/)
(Free) online spherical 3D plot software: MathStudio (http://mathstud.io/)
(Free) offline math calculation software: R
Microsoft Excel, Power Point, Word.
Public TV's space science related programs: PBS-NOVA, BBC-documentary, National Geographic-documentary, etc.
Journal: Scientific American.

Note: I am still looking for endorsers to post all my SunQM papers (including the future papers) to arXiv.org. Thank you in advance!

Note: With my 31 of SunQM papers that have been posted out so far, I believe that the framework of the {N,n} QM has been fully established. It is clear now that the {N,n} QM description is not only suitable for the mass field, but also suitable for the force field (or the energy field, etc.). Thus, my (10 years of closed-door) research phase on the {N,n} QM will be ended in about one year (most likely in the summer of 2024). After that, I will re-write the SunQM papers (~ 35 of them) in the form of a text book.

Appendix A. Using $\mathbf{v_{n,ph}} = \frac{\mathbf{n}}{\mathbf{2}}\mathbf{v_{n,gr}}$ to update SunQM-6s1's eq-1 through eq-20

$v_{classical} = v_{gr} = \frac{2}{n} v_{ph}$ SunQM-6s1's-updated-eq-1

1) Bohr atom's particle description version:

$F_e = \frac{1}{4\pi\epsilon_0}\frac{q^2}{{r_n}^2}$, $F_c = m\frac{{v_n}^2}{r_n}$, $F_e = F_c$, $\frac{1}{4\pi\epsilon_0}\frac{q^2}{{r_n}^2} = m\frac{{v_n}^2}{r_n}$, or $v_n = \sqrt{\frac{1}{4\pi\epsilon_0}\frac{q^2}{r_n m}}$, SunQM-6s1's-updated-eq-2

$E_n = K_n + V_n = \frac{1}{2}m{v_n}^2 - \frac{1}{4\pi\epsilon_0}\frac{q^2}{r_n} = \frac{1}{2}m{v_n}^2 - m{v_n}^2 = \frac{-1}{2}m{v_n}^2$, SunQM-6s1's-updated-eq-3

$v_{n,gr} = \frac{v_{1,gr}}{n}$, known from traditional QM, SunQM-6s1's-updated-eq-4

$\lambda_{n,gr} = n\lambda_{1,gr}$, defined from Bohr Model's and de Broglie wave, SunQM-6s1's-updated-eq-5

$v_{n,gr} = n\lambda_{n,gr}f_{n,gr}$ SunQM-6s1's-updated-eq-6

$f_{n,gr} = \frac{f_{1,gr}}{n^3}$, SunQM-6s1's-updated-eq-7

$E_n - E_{n'} = \frac{-1}{2}m{v_n}^2 - \frac{-1}{2}m{v_{n'}}^2 = \frac{-1}{2}m{v_1}^2\left(\frac{1}{n^2} - \frac{1}{n'^2}\right)$, SunQM-6s1's-updated-eq-8

2) Bohr atom's (de Broglie) matter wave description version:

$\lambda_{n,ph} = 2\pi r_n$ SunQM-6s1's-updated-eq-9

$\lambda_{n,ph} = n^2\lambda_{1,ph}$, or, $\lambda_{n,ph} = 2\pi r_1 n^2$ SunQM-6s1's-updated-eq-10

$v_{n,ph} = \lambda_n f_{n,ph}$. SunQM-6s1's-updated-eq-11

$f_{n,ph} = \frac{v_{n,ph}}{\lambda_{n,ph}} = \frac{n}{2}\frac{v_{n,gr}}{n\lambda_{n,gr}} = \frac{n}{2}f_{n,gr}$ SunQM-6s1's-updated-eq-12

$E_n = -Hmf_{n,ph}$, SunQM-6s1's-updated-eq-13

$v_{n,ph} = v_{1,ph}$ SunQM-6s1's-updated-eq-14

$f_{n,ph} = f_{1,ph}/n^2$ SunQM-6s1's-updated-eq-15

$2\pi f_{n,ph} = \omega_{n,ph}$, SunQM-6s1's-updated-eq-16

$E_n - E_{n'} = -Hmf_{n,ph} - Hmf_{n',ph} = -Hmf_{1,ph}\left(\frac{1}{n^2} - \frac{1}{n'^2}\right)$, SunQM-6s1's-updated-eq-17

$\Delta f_{n\to n',ph} = f_{n',ph} - f_{n,ph} = f_{1,ph}\left(\frac{1}{n'^2} - \frac{1}{n^2}\right)$, deduced, SunQM-6s1's-updated-eq-18

$\lambda_{n\to n'} = \frac{c}{f_{n,ph} - f_{n',ph}} = \frac{c}{f_{1,ph}\left(\frac{1}{n^2} - \frac{1}{n'^2}\right)}$ SunQM-6s1's-updated-eq-19

$f_{n,ph} = \frac{n}{2}f_{n,gr}$ SunQM-6s1's-updated-eq-20

Appendix B. Using $v_{n,ph} = \frac{n}{2}v_{n,gr}$ to re-deduce equations in SunQM-4's section I-c.

$\Psi_k(x,t) = Ae^{\left[i\left(kx - \frac{\hbar k^2}{2m'}t\right)\right]} = Ae^{\left[i\left(kx - \frac{E}{\hbar}t\right)\right]} = Ae^{[i(px-Et)/\hbar]}$ SunQM-4's-updated-eq-19

$E_{\varphi,j} = K_{\varphi,j} + V_{\varphi,j} = K_{\varphi,j} = \frac{1}{2}m'{v_j}^2$ SunQM-4's-updated-eq-20

$E_n = E_{r\theta\varphi,n} = \frac{-1}{2}m'{v_{n,gr}}^2$ SunQM-4's-updated-eq-21

$T(t) \propto e^{-i\frac{E_{\varphi,j}}{\hbar}t}$ SunQM-4's-updated-eq-22

$T(t) \propto e^{-i\frac{E_{\varphi,j}}{\hbar_{gen}}t}$ SunQM-4's-updated-eq-23

$E_{\varphi,j} = Hm'f_{j,ph} = h_{gen}f_{j,ph}$ SunQM-4's-updated-eq-24

$T(t) \propto e^{-i\frac{E_{\varphi,j}}{\hbar_{gen}}t} = e^{-i\frac{h_{gen}f_{j,ph}}{\hbar_{gen}}t} = e^{-i2\pi f_{j,ph}t}$ SunQM-4's-updated-eq-25

$2\pi f_{j,ph} = \omega_{j,ph}$ SunQM-4's-updated-eq-26

$2\pi f_{n,ph} = \omega_{n,ph}$ SunQM-4's-updated-eq-27

$T(t) \propto e^{-i\frac{E_{\varphi,j}}{\hbar_{gen}}t} = e^{-i2\pi f_{n,ph}t}$ SunQM-4's-updated-eq-28

$H_n = \frac{2\pi}{n}\sqrt{GMr_n}$ SunQM-4's-updated-eq-29

$$\frac{E_{\varphi,j}}{\hbar_{gen}} = \frac{\frac{1}{2}m\prime {v_{n,gr}}^2}{\frac{H_n m\prime}{2\pi}} = \frac{\pi {v_{n,gr}}^2}{H_n} = \frac{\pi {v_{n,gr}}^2}{\frac{2\pi\sqrt{GMr_n}}{n}} = \frac{n}{2}\frac{{v_{n,gr}}^2}{v_{n,gr}r_n} = \left(\frac{n}{2}\right)\frac{v_{n,gr}}{r_n}$$ SunQM-4's-updated-eq-30

$$2\pi f_{n,ph} = \left(\frac{n}{2}\right)\frac{v_{n,gr}}{r_n} = \omega_{n,ph}$$ SunQM-4's-updated-eq-31

$$\Psi_k(x,t) = Ae^{\left[i\left(kx-\frac{E}{\hbar}t\right)\right]} = Ae^{i(kx-\omega_{n.ph}t)} = Ae^{ikx}e^{-i\omega_{n,ph}t}$$ SunQM-4's-updated-eq-32

$$T(t) \propto e^{-i\omega_{n,ph}t}$$ SunQM-4's-updated-eq-33

$$\frac{v_{n,gr}}{r_n} = \omega_{n,gr} = \omega_{n,gr}$$ SunQM-4's-updated-eq-34

$$v_{classical} = v_{gr} = \frac{2}{n}v_{ph}$$ SunQM-4's-updated-eq-35

$$v_{classical} = v_n = v_{n,gr} = \frac{2}{n}v_{n,ph}$$ SunQM-4's-updated-eq-36

$$v_{n,ph} = \lambda_{n,ph}f_{n,ph}$$ SunQM-4's-updated-eq-37

$$\omega_{n,ph} = 2\pi f_{n,ph} = \left(\frac{n}{2}\right)\frac{v_{n,gr}}{r_n} = \frac{v_{n,ph}}{r_n}$$ SunQM-4's-updated-eq-38

$$\omega_n = \omega_{n,gr} = \frac{v_{n,gr}}{r_n} = \frac{v_n}{r_n}$$ SunQM-4's-updated-eq-39

$$\boldsymbol{\omega_{n,ph}} = 2\pi f_{n,ph} = \left(\frac{n}{2}\right)\frac{v_{n,gr}}{r_n} = \left(\frac{n}{2}\right)\omega_{n,gr} = \left(\frac{\mathbf{n}}{\mathbf{2}}\right)\boldsymbol{\omega_{n,gr}}$$ SunQM-4's-updated-eq-**40**

$$\omega_{n,ph} = \frac{\omega_{n,gr}}{2}$$ SunQM-4's-updated-eq-41

Appendix C. Integration of elliptical orbital angular momentum between r_n and r_{n+1} within n shell

Analytical equation of an ellipse centered at the origin with width 2a and height 2b is: $\frac{x^2}{a^2}+\frac{y^2}{b^2}=1$. If a ≥ b, the foci are at (±c, 0) with $c=\sqrt{a^2-b^2}$, eccentricity $e=\frac{c}{a}$. Then, polar equation of the ellipse with one focus at the origin and the other at the positive real axis is $r=\frac{a(1-e^2)}{1-e\cos(\theta)}$, the average radius can be calculated by using the integral $\frac{1}{2\pi}\int_0^{2\pi} r(\theta)\ d\theta$. (https://math.stackexchange.com/questions/3107249/the-average-radius-of-an-ellipse#:~:text=which%20gives%20r%3D%E2%88%9Aa,r%3Da%2Bb2). For an elliptical orbital angular momentum within n shell (with the perihelion at r_n and the aphelion at r_{n+1}), eq-27 can be re-written as, $\left|\vec{\mathbf{L}}_{\mathbf{n,orbit}}\right| = mv_nr_n = (mv_1r_1)n = (mv_1r_1)\sqrt{\frac{r_n}{r_1}} = \sqrt{\frac{r_n}{r_1}}\hbar$, where both r_1 and $\hbar = mv_1r_1$ are the fixed values, and $r_n = r(\theta)$ is the only variable. Then, using the integration

$$\frac{1}{2\pi}\int_0^{2\pi}\left|\vec{\mathbf{L}}_{\mathbf{n,orbit}}\right|\ d\theta = \frac{1}{2\pi}\int_0^{2\pi}\sqrt{\frac{r_n}{r_1}}\hbar\ d\theta = \frac{\hbar}{2\pi}\int_0^{2\pi}\sqrt{\frac{r(\theta)}{r_1}}\ d\theta = \frac{\hbar}{2\pi}\int_0^{2\pi}\sqrt{\frac{a(1-e^2)}{(1-e\cos(\theta))r_1}}\ d\theta$$ eq-29

we can calculate out the averaged $\left|\vec{\mathbf{L}}_{\mathbf{n,orbit}}\right|$ for an elliptical orbital motion within n shell (from r_n to r_{n+1}).

For n = 1 shell between r_1 and $r_2 = 4r_1$, the elliptical orbit's a = $(r_1 + 4r_1)/2 = (5/2)r_1 = 2.5r_1$, c = $(5r_1 - 2r_1)/2 = (3/2)r_1$, e = $[(3/2)r_1]/[(5/2)r_1] = (3/5) = 0.6$. $\frac{1}{2\pi}\int_0^{2\pi}\left|\vec{\mathbf{L}}_{\mathbf{n=1,orbit}}\right|\ d\theta = \frac{\hbar}{2\pi}\int_0^{2\pi}\sqrt{\frac{2.5r_1(1-0.6^2)}{(1-0.6\cos(\theta))r_1}}\ d\theta = \frac{\hbar}{2\pi}\int_0^{2\pi}\sqrt{\frac{2.5(1-0.6^2)}{1-0.6\cos(\theta)}}\ d\theta = 1.37\hbar$, it is close (but not equals) to (n + ½)$\hbar$ = 1.5$\hbar$.

For n = 2 shell between $r_2 = 4r_1$, and $r_3 = 9r_1$, the elliptical orbit's a = $(4r_1 + 9r_1)/2 = (13/2)r_1 = 6.5r_1$, c = $(13r_1 - 2\times4r_1)/2 = (5/2)r_1$, e = c/a = (5/13). $\frac{1}{2\pi}\int_0^{2\pi}\left|\vec{\mathbf{L}}_{\mathbf{n=2,orbit}}\right|\ d\theta = 2.42\hbar$, it is ≤ (n + ½)$\hbar$ = 2.5$\hbar$.

For n = 3 shell, a = $12.5r_1$, c = $(7/2)r_1$, e = 7/25, $\frac{1}{2\pi}\int_0^{2\pi}\left|\vec{\mathbf{L}}_{\mathbf{n=3,orbit}}\right|\ d\theta = 3.45\hbar$, it is ≤ (n + ½)$\hbar$ = 3.5$\hbar$.

For n = 36 shell between $r_{36} = 36*36r_1$ and $r_{37} = 37*37r_1$, the elliptical orbit's a = $(36*36r_1 + 37*37r_1)/2 = (2665/2)r_1 = 1332.5r_1$, c = $(2665r_1 - 2*36*36r_1)/2 = (73/2)r_1$, e = $[(73/2)r_1]/[(2665/2)r_1] = (73/2665)$. Then, $\frac{1}{2\pi}\int_0^{2\pi}\left|\vec{\mathbf{L}}_{\mathbf{n=36,orbit}}\right|\ d\theta =$

$\frac{\hbar}{2\pi}\int_0^{2\pi}\sqrt{\frac{1332.5\left(1-\left(\frac{73}{2665}\right)^2\right)}{1-\frac{73}{2665}\cos(\theta)}}\,d\theta = 36.4949\hbar$, it is very close to (n + ½)$\hbar$ = 36.5$\hbar$. The "Wolfram Alpha" calculations are shown in below:

$\int_0^{2\pi}\frac{\sqrt{\frac{2.5(1-0.6\cdot 0.6)}{1-0.6\cos(x)}}}{2\pi}dx = 1.37288$, $\int_0^{2\pi}\frac{\sqrt{\frac{6.5\left(1-\left(\frac{5}{13}\right)^2\right)}{1-\frac{5\cos(x)}{13}}}}{2\pi}dx = 2.42456$, $\int_0^{2\pi}\frac{\sqrt{\frac{12.5\left(1-\left(\frac{7}{25}\right)^2\right)}{1-\frac{7\cos(x)}{25}}}}{2\pi}dx = 3.44627$, $\int_0^{2\pi}\frac{\sqrt{\frac{1332.5\left(1-\left(\frac{73}{2665}\right)^2\right)}{1-\frac{73\cos(x)}{2665}}}}{2\pi}dx = 36.4949$

Appendix D. Construction of Schrodinger equation's solution for a proton-electron system (in an H-atom)

(Note: This is a citizen-scientist-leveled work, only for myself to read). If it is in nLL mode (and with high n'), then we can use SunQM-3s11's eq-45 for the planet, SunQM-3s11's eq-5 for the Sun, and SunQM-3s11's eq-65 for the superposition. (Alternatively, we can use SunQM-4's eq-44 for the planet, SunQM-4's eq-63 for the Sun, SunQM-4's eq-80 for the superposition. But it is too complicated, and is ignored here).

$$r^2\,|\Psi(r,\theta,\phi-\omega t)_{Planet}|^2 \propto \left(\frac{r}{r_n}e^{\left(1-\frac{r}{r_n}\right)}\right)^{2n}\sin(\theta)^{2(n-1)}\cos(\varphi-\omega t)^{2(n-1)} \qquad \text{eq-30 (SunQM-3s11's eq-45)}$$

For the electron, if use n=1 as the base n, and use Bohr radial $a_0 = r_1$, then $r^2\,|\Psi(r,\theta,\phi-\omega t)_{electron}|^2 \propto \left(\frac{r}{r_n}e^{\left(1-\frac{r}{r_n}\right)}\right)^{2n}\sin(\theta)^{2(n-1)}\cos(\varphi-\omega t)^{2(n-1)} = \left(\frac{r}{a_0}e^{\left(1-\frac{r}{a_0}\right)}\right)^{2}$. It is not a nLL mode, because the n=1 QM state is always doing 100% RF movement. It lost the orbital angular-speed (and the spin-speed) information of $(\varphi-\omega t)$. If we force x'y'z' coordinate (or the correlated r'θ'φ' coordinate) to do the same RF as the n=1 electron's RF movement, so that the trajectory of electron's orbit is forced to be fixed in the x'y'-2D plane, and proton's spin axis is force to be fixed along +z' axis, then it is a nLL mode, it forced $\sin(\theta')^{2(n-1)} = 1$, but still retained $\cos(\varphi'-\omega t)^{2(n-1)}$. Therefore, it may retain electron's orbital angular-speed (and the spin-speed) information of $(\varphi'-\omega t)$.

Then, we need to use the high-frequency n', with the Eigen description of an electron size at {-17,1//6}, (see SunQM-7's Table-1). Now let's use {-17,1//6} size (or the electron size) as r_1, and define a new interior {N,n//6} QM system as **elec{0,1//6}**. Then, elec{0,1//6} ≈ Sun{-17,1//6} ≈ prot{-2,1//6} ≈ e1{-5,1//6}.

Notice that atomic n=1 orbit is in the {-12,1//6}o orbital space, which equals to the {-13,n=6..11//6}o orbital space, or {-12,1//6}o = {-13,n=6..11//6}o = {-14,n=(6..11)*6//6^2}o = {-15,n=(6..11)*6^2//6^3}o = {-16,n=(6..11)*6^3//6^4}o = {-17,n=(6..11)*6^4//6^5}o orbital spaces. So, if using elec{0,1//6} ≈ Sun{-17,1//6} to mimic the electron's size, then the atomic n=1 orbital space e1{0,1//6}o should have a high-frequency n' collection from n' = 6*6^4 = 1*6^5 to n' = 12*6^4 -1 = (2*6^5) - 1. Using eq-30, it becomes

$$r'^2\left|\Psi(r',\theta',\phi'-\omega t)_{electron,n=1}\right|^2 \approx \sum_{n'=6\hat{}5}^{n'=2\times 6\hat{}5-1}\left[\left(\frac{r'}{r'_{n'}}e^{\left(1-\frac{r'}{r'_{n'}}\right)}\right)^{2n'}\sin(\theta')^{2(n'-1)}\cos(\varphi'-\omega t)^{2(n'-1)}\right] \qquad \text{eq-31}$$

where ω is the orbital angular-speed of the n =1 electron in the H-atom (with the $r'_1 = a_0 = 5.29E\text{-}11$ meters and $v_{n=1} = 2.19E+6$ m/s). (Note: According to SunQM-4's-updated-eq-32, this ω should be ω_{ph}). This is the Eigen description, with the BP (or NBP) density size that is the same as the size of an electron (i.e., the size of {-17,1//6}), with the collective (of all circular and elliptical) orbital trajectories cover all of the atomic n=1 orbital space (i.e., the orbital space of {-12,1//6}o = {-17, n=(1*6^5.. (2*6^5)-1)//6^5}), and with the retained electron's spin-speed as well as the orbital angular-speed information of $(\varphi'-\omega t)$. This Schrodinger equation's solution may also contain the electron's spin information (as the positive/negative peaks of the NBP, or the wave function). Notice that this is in the RF-eliminated x'y'z' coordinate with nLL mode. In theory

(or only in imagination?), we may can put x'y'z' (or r'θ'φ') back into the RF-retained xyz (or rθφ) coordinate, and obtain the atomic n=1 electron's spin information at 100% RF state.

For the proton in the H-atom, also using the electron size {-17,1//6} = elec{0,1//6} ≈ prot{-2,1//6} ≈ e1{-5,1//6} as r_1, then prot{0,1//6} = elec{2,1//6} = elec{0,36//6} in size, that means the size of a proton prot{0,1//6} can be described within the orbital space of elec{0,n=1..35//6}o. Then, the proton's Born probability density function may can be described as

$$r'^2 \left|\Psi(r',\theta',\phi'-\omega t)_{proton}\right|^2 \approx \sum_{n'=1}^{n'=6\wedge 2-1}\left[\left(\frac{r'}{r'_{n'}}e^{\left(1-\frac{r'}{r'_{n'}}\right)}\right)^{2n'}\sin(\theta')^{2(n'-1)}\cos(\varphi'-\omega t)^{2(n'-1)}\right] \qquad \text{eq-32}$$

where ω is the same as that in eq-31, and it is the spin-speed of both the electron's and the proton's (in the H-atom). Notice that eq-32 is also in the (RF motion eliminated) x'y'z' coordinate, and both the proton and electron are doing nLL mode movement in this coordinate.

Notice that in both eq-31 and eq-32, the motion in r'-1D is in the (bi-directional) steady state (with either r = a_0 for electron's orbit, or $r_{n'=1} \le r < r_{n'=36}$ for the proton's size), so it is described with Born probability $\left(\frac{r'}{r'_{n'}}e^{\left(1-\frac{r'}{r'_{n'}}\right)}\right)^{2n'}$; the motion in θ'-1D is also in the (bi-directional) steady state (with θ' = π/2), so it is also described with Born probability $\sin(\theta')^{2(n'-1)}$; however, the motion in φ'-1D is in the uni-direction, it is always rotating with $\varphi' = \omega t$, so it is described with the non-Born probability (NBP) as $\cos(\varphi'-\omega t)^{2(n'-1)}$ that uses only half circle within $-\pi/2 < (\varphi'-\omega t) \le +\pi/2$. (Note: the same explanation should also can be applied to the similar equations in SunQM-3s11 and in SunQM-4).